

1 Reviews and syntheses: Opportunities for robust use of peak 2 intensities from high resolution mass spectrometry in organic 3 matter studies

4 William Kew¹, Allison Myers-Pigg², Christine H. Chang², Sean M. Colby², Josie Eder¹, Malak
5 M. Tfaily³, Jeffrey Hawkes⁴, Rosalie K. Chu¹, James C. Stegen^{2,5*}

6 ¹Environmental Molecular Sciences Laboratory, Richland, WA 99352, USA

7 ²Pacific Northwest National Laboratory, Richland, WA 99352, USA

8 ³Department of Environmental Science, University of Arizona, Tucson, AZ, 85719, USA

9 ⁴Department of Chemistry, University of Uppsala, Uppsala, 75124, Sweden

10 ⁵School of the Environment, Washington State University, Pullman, WA, 99164, USA

11 *Correspondence to: James C. Stegen (James.Stegen@pnl.gov)

12 **Abstract** Earth's biogeochemical cycles are intimately tied to the biotic and abiotic processing of organic matter
13 (OM). Spatial and temporal variation in OM chemistry is often studied using direct infusion, high resolution Fourier
14 transform mass spectrometry (FTMS). An increasingly common approach is to use ecological metrics (e.g., within-
15 sample diversity) to summarize high-dimensional FTMS data, notably Fourier transform ion cyclotron resonance
16 MS (FTICR MS). However, problems can arise when FTMS peak intensity data are used in a way that is analogous
17 to abundances in ecological analyses (e.g., species abundance distributions). Using peak intensity data in this way
18 requires the assumption that intensities act as direct proxies for concentrations. Here we show that comparisons of
19 the same peak across samples (within-peak) may carry information regarding variation in relative concentration, but
20 comparing different peaks (between-peak) within or between samples does not. We further developed a simulation
21 model to study the quantitative implications of using peak intensities to compute ecological metrics (e.g., [intensity-
22 weighted mean properties and diversity](#)) that rely on information about both within-peak and between-peak shifts in
23 relative abundance. We found that despite analytical limitations of linking concentration to intensity, the ecological
24 metrics often perform well in terms of providing robust qualitative inferences and sometimes quantitatively-accurate
25 estimates of diversity and [mean](#) molecular characteristics. We conclude with recommendations for robust use of
26 peak intensities for natural organic matter studies. A primary recommendation is the use and extension of the
27 simulation model to provide objective guidance on the degree to which conceptual and quantitative inferences can
28 be made for a given analysis of a given dataset. Broad use of this approach can help ensure rigorous scientific
29 outcomes from the use of FTMS peak intensities in environmental applications.

33 1 Introduction

34 Organic matter (OM) plays a central role in Earth's biogeochemical cycles, and is both a resource for and product of
35 metabolism. The detailed chemistry of OM (e.g., nominal oxidation state) can modulate and reflect biogeochemical
36 rates and fluxes within and across ecosystems (e.g., [LaRowe and Van Cappellen, 2011](#); [Boye et al., 2017](#);
37 [Garayburu-Caruso et al., 2020](#)), ([Boye et al., 2017](#); [Garayburu-Caruso et al., 2020](#); e.g., [LaRowe and Van Cappellen,
38 2011](#)), yet our understanding of this complexity is limited by our analytical abilities to view it ([Steen et al., 2020](#);
39 [Hedges et al., 2000](#); [Hawkes and Kew, 2020a](#)), ([Hawkes and Kew, 2020a](#); [Hedges et al., 2000](#); [Steen et al., 2020](#)).
40 Given the importance of OM chemistry to biogeochemical cycling, there is a need to understand how and why that
41 chemistry varies through space and time. To help meet this need, there has been growing interest in using concepts
42 and methods from ecology to study the chemogeography and chemodiversity of OM in a variety of ecosystems (e.g.,

Formatted: Header

Style Definition: Heading 1

Style Definition: Heading 2

Style Definition: Heading 3

Style Definition: Heading 4

Style Definition: Heading 5

Style Definition: Heading 6

Style Definition: Title

Style Definition: Subtitle

43 [Kujawinski et al., 2009](#); [Kellerman et al., 2014](#); [Tanentzap et al., 2019](#); [Danezak et al., 2021](#));([Danczak et al., 2021](#);
44 [Kellerman et al., 2014](#); e.g., [Kujawinski et al., 2009](#); [Tanentzap et al., 2019](#)). This is a promising approach as there
45 are many conceptual parallels between the chemical species that comprise OM and the biological species that
46 comprise ecological communities ([Danezak et al., 2020](#));([Danczak et al., 2020](#)).

47
48 The most fundamental ecological data type is the species-by-site matrix. This matrix indicates how many individuals
49 of each species occur in each sampled community. Ecologists use species-by-site matrices to ask myriad questions
50 related to biological diversity, and often complement these data with information on the properties or 'functional
51 traits' of species (e.g., body size) (McGill et al., 2006; Villéger et al., 2017; Violle et al., 2007). Two common
52 analyses are known as α -diversity and β -diversity, each with numerous metrics ([Whittaker, 1972](#); [Anderson et al.,](#)
53 [2014](#));([Anderson et al., 2011](#); [Whittaker, 1972](#)), including versions that include functional trait information
54 (Laliberté and Legendre, 2010). α -diversity measures the diversity within a given community. β -diversity has been
55 variously defined, but essentially measures variation in composition across communities. Both α -diversity and β -
56 diversity can be quantified using presence-absence data or they can include estimates of each species' relative
57 abundance within and between communities (Fig. 1). In addition to being incorporated into these diversity metrics,
58 functional trait data can be used to estimate community-level mean trait values (Lavorel et al., 2008). As with
59 diversity, mean trait values can be estimated using presence-absence or relative abundance data. Estimates of
60 diversity and mean trait values are examples of ecological metrics often applied to OM chemistry (Bahureksa et al.,
61 2021; Cooper et al., 2022; Sakas et al., 2024; Tanentzap et al., 2019).

62
63 The chemistry of OM is commonly studied using high resolution Fourier transform mass spectrometry (FTMS)
64 techniques (e.g., [Hawkes and Kew, 2020b](#));(e.g., [Hawkes and Kew, 2020b](#)), such as Orbitrap or Ion Cyclotron
65 Resonance (ICR) MS, via direct infusion of samples. At present, the highest resolution approach for untargeted
66 analysis of OM is via a 21 Tesla FTICR MS ([Marshall et al., 1998](#); [Shaw et al., 2016](#); [Smith et al., 2018](#); [Bahureksa](#)
67 [et al., 2021](#));([Bahureksa et al., 2021](#); [Marshall et al., 1998](#); [Shaw et al., 2016](#); [Smith et al., 2018](#)). The output data
68 produced is a spectrum containing peaks represented by a signal intensity (Fig. 2 y-axis) and a mass-to-charge ratio
69 (m/z) (Fig. 2 x-axis), which is equivalent to the mass for singly charged ions as routinely detected in natural organic
70 matter (NOM) measurements. In turn, regardless of the type of MS instrument used, the MS data inherently lead to
71 an OM peak-by-sample data matrix, akin to an ecological species-by-site data matrix. The high resolution data from
72 MS often results in a large matrix, wherein a single sample may contain thousands to tens of thousands of peaks. It
73 is often possible to assign molecular formulas to a large fraction of observed peaks, which enables calculation of
74 several properties such as stoichiometric ratios (Bahureksa et al., 2021; Cooper et al., 2022) that are akin to
75 organismal functional traits. To take advantage of these rich data, FTMS data have been analyzed using the same α -
76 diversity and, β -diversity, and mean trait metrics that are commonly used by ecologists to study biological diversity
77 (e.g., [Kellerman et al., 2014](#));communities (e.g., Kellerman et al., 2014). Such analyses are exciting, as they enable
78 the same conceptual questions and quantitative frameworks to be applied to biological (e.g., microbial communities)
79 and chemical (i.e., OMNOM) components that directly interact with each other within ecosystems ([Lucas et al.,](#)
80 [2016](#); [Osterholz et al., 2016](#); [Li et al., 2018](#); [Tanentzap et al., 2019](#); [Danezak et al., 2020, 2021](#));([Danczak et al.,](#)
81 [2020, 2021](#); [Li et al., 2018](#); [Lucas et al., 2016](#); [Osterholz et al., 2016](#); [Tanentzap et al., 2019](#)).

82
83 The use of ecological metrics with MS data is particularly common with FTMS datasets and there is great potential
84 to continue leveraging concepts from ecology in high-resolution OMNOM analyses. Care is required, however, in
85 using FTMS peak intensity data to estimate α -diversity, β -diversity, mean trait values, and related ecological
86 analyses (e.g., 'species' abundance distributions). Key to these ecological analyses is the assumption that within
87 complex NOM samples, differences in peak intensity are proportional to differences in concentrations of the
88 associated molecules. Studies using FTMS often avoid using peak intensities due to uncertainties in whether it is
89 valid to assume proportionality between peak intensities and concentrations within and across NOM samples
90 ([Kujawinski, 2002](#));([Bhatia et al., 2010](#); [Danczak et al., 2020](#); [Kujawinski, 2002](#)). These studies may be discarding
91 useful information, though it is unclear what biases and uncertainties are introduced into ecological metrics when

92 using FTMS peak intensities. To help advance robust use of FTMS datasets for NOM studies, we review the
93 theoretical reasons why peak intensities may not reflect true concentrations, provide empirical evaluation of this
94 theory, and invoke *in silico* simulation to quantify the associated impacts on ~~ecological~~ecology-inspired analyses.
95 While theory and empirical analyses demonstrate disconnects between peak intensities and concentrations in FTMS
96 data, the simulations show that intensity-weighted ecological metrics ~~are often still~~ provide robust estimates of NOM
97 diversity and mean trait values. We end with practical recommendations and propose a path forward for increasing
98 robust use of FTMS peak intensities for NOM studies.

99 2 Theoretical Foundations

100 Here we provide a review of the theoretical foundations behind why assuming proportionality between peak
101 intensities and concentrations in FTMS can be challenging. This section will be of most value to FTMS data users
102 that are not formally trained in mass spectrometry, and serves as a review of mass spectrometry principles (~~see also~~
103 Kujawinski, 2002; Urban, 2016; Bahureksa et al., 2021); (~~Bahureksa et al., 2021~~; see also Kujawinski, 2002; Urban,
104 2016). We focus on FTMS (i.e., FTICR and Orbitrap), but many of the principles are applicable across all MS
105 platforms. We highlight three considerations: ionization, ion transfer, and ion signal detection in the context of
106 commercial FTMS instruments. These considerations have practical implications tied to within-peak and between-
107 peak comparisons (Fig. 2). Here, we define ‘within-peak’ as comparing peak intensities of the same feature (i.e., m/z
108 or molecular formula) across different sample spectra and ‘between-peak’ as comparing peak intensities across
109 different features. Both within-peak and between-peak comparisons are fundamentally based on the m/z observed
110 within a mass spectrum and neither address comparisons across isomers. Further, we suggest consistent use of the
111 term ‘intensity’ in FTMS NOM studies to describe how much signal is observed for a given peak, as opposed to
112 ‘height’, ‘magnitude’, or other alternatives. While terminology is not our central focus, it is useful to pursue
113 consistency across studies. As discussed below, within-peak comparisons can be robust under certain situations, but
114 there are limitations with between-peak comparisons that may be unavoidable. The following discussion is not an
115 exhaustive treatment of all decisions associated with a complete FTMS experiment, and we do not deeply address
116 factors such as sample preparation, choice of ionization mode, and instrument specific parameter optimization.
117 These topics have been discussed in a recent review (~~Bahureksa et al., 2021~~); (~~Bahureksa et al., 2021~~).

118 2.1 Ionization Efficiency and Isomers

119 Electrospray ionization (ESI) is the most common technique for generating ions from NOM samples. When using
120 ESI, the peak intensity for any given molecular mass (or molecular formula) will depend on both concentration and
121 ionization efficiency, the latter of which is dependent on structure, pKa, and the other molecules in the sample
122 (~~Kruve et al., 2014~~); (Kruve et al., 2014). In NOM samples, one detected mass or peak combines signals from
123 multiple isomers which all have the same molecular formula but different structures. The different structures impact
124 ionization efficiency, but FTMS data contains no information about this structural variation. Unfortunately, to date,
125 no liquid chromatography (~~Kim et al., 2019; Han et al., 2021~~) or ion mobility separation (~~Tose et al., 2018; Leyva et~~
126 ~~al., 2020~~); (Han et al., 2021; Kim et al., 2019) or ion mobility separation (Leyva et al., 2020; Tose et al., 2018)
127 technique has yet demonstrated sufficient resolution to completely infer structural variation among isomers within
128 complex NOM samples. Unknown variation in structure can, therefore, lead to unknown variation in peak
129 intensities. This challenge can be compounded by ionization suppression that occurs when the ionization efficiency
130 of one type of molecule (i.e., peak) is altered by the presence of other types of molecules (~~Ruddy et al.,~~
131 ~~2018~~); (Ruddy et al., 2018). Ionization suppression can be mitigated by online separation whereby non-targeted LC-
132 MS approaches may yield more quantitative data (~~Kruve, 2020~~); (Kruve, 2020), but matrix effects remain a
133 significant issue even for LC-MS (~~Trufelli et al., 2011~~); (Trufelli et al., 2011). In NOM samples with thousands of
134 types of organic molecules, the molecular interactions likely have complex influences over realized ionization
135 efficiencies. While it is possible to control for some of these challenges (e.g., using consistent sample concentrations
136 and preparations), many additional factors (e.g. molecular structures, pKas, and interactions among molecules in

137 NOM samples) cannot yet be accounted for. Interpretation of peak intensities as proxies for concentrations in FTMS
138 datastreams may, therefore, be prone to uncertainty.

139 2.2 Ion transmission and collection

140 In FTMS, packets of ions are accumulated in a trap prior to their transmission to the analyzer cell ([Fig. 3 Panel A](#)
141 [section d; Senko et al., 1997; Makarov et al., 2006](#))([Makarov et al., 2006; Fig. 3 Panel A section d; Senko et al.,](#)
142 [1997](#)). The duration of time in which ions are accumulated is often varied to yield an optimal ion population for the
143 analyzer cell. The duration of this event can change the relative abundance, and thus observed peak intensities of
144 different ions ([Cao et al., 2016](#))([Cao et al., 2016](#)). Increases in the true abundance of other ions can decrease the
145 measured peak intensity of a given ion due to a dilution effect resulting from a finite number of ions that can fit
146 within the ion trap. Additional challenges arise due to variation in the speed at which different ions move from the
147 accumulation trap and into the analysis cell. Smaller ions move more quickly and therefore reach the analysis cell
148 sooner than larger ions. Variation in the accumulation time across samples and FTMS instruments, combined with
149 among-ion variation in transmission speed, can introduce additional uncertainty in the relationship between peak
150 intensities and true concentrations.

151 2.3 Ion signal detection

152 The final step in data collection via FTMS is signal detection. The intensity of the signal is proportional to the
153 abundance of a given ion in the analysis cell, the proximity of ions to the detector ([Kaiser et al., 2013](#)), and the ion
154 charge state ([Wörner et al., 2020](#))([Kaiser et al., 2013](#)), and the ion charge state ([Wörner et al., 2020](#)). Similar to
155 molecular interactions impacting ionization efficiencies, different types of ions can interact to affect each other's
156 signal intensity. The Fourier transform applied to the data also complicates extremely accurate relative
157 quantification of ion abundance between peaks ([Makarov et al., 2019](#))([Makarov et al., 2019](#)). These challenges at
158 the detection stage can add more uncertainty to the relationship between peak intensity and concentrations,
159 particularly for complex NOM samples.

160

161 3 Empirical Evaluations

162

163 In this section, we move beyond theoretical considerations to empirical evaluations of the real-world relationships
164 between peak intensities and concentrations. Similar to above, this section will be of primary value to those without
165 formal training as mass spectrometrists, but who use FTMS data to study NOM. [The experimental methods used are](#)
166 [described in detail in the Supplementary Information.](#)

167 3.1 Direct comparison of peak intensities in idealized samples

168 As discussed above, different organic compounds ionize with different efficiencies. In theory, this may lead to
169 variation in observed peak intensities even when all organic compounds have the same true concentration. To
170 evaluate this theoretical expectation, we analyzed several different types of organic compounds in different
171 conditions via FTICR-MS. We selected chemical standards ([see Supplementary Information for details](#)) which are
172 natural products with molecular formula and chemistries typical of compounds commonly observed in organic
173 matter, and were amenable to negative mode ESI analysis. First, we analyzed three separate dilution ladders of
174 individual pure compounds dissolved in pure methanol. These standards were analyzed at higher concentrations than
175 typically observed for NOM because they were single compounds rather than formula-summed features (with
176 multiple isomers) within a NOM spectrum; higher concentrations were required to compensate for lower isomeric
177 diversity. These three compounds gave rise to different peak intensities under otherwise identical conditions (Fig.
178 4A). Trehalose, for example, had much lower peak intensity than sinapic acid at the same actual concentration. The
179 difference in signal intensity was also apparent amongst compounds that ionize well under negative mode ESI; for
180 example, two different structures containing the same number of carboxylic acid units exhibited differences in signal

181 intensity. We also observed differences in peak intensities amongst structural isomers (i.e., same molecular formula
182 and mass) (Fig. 4B). Each peak observed via direct infusion FTICR-MS may be several isomers. These isomers may
183 be observable through chromatographic separation (Kim et al., 2019), ion mobility separations
184 (Leyva et al., 2019), or by statistical inference of tandem mass spectrometry (Zark et al.,
185 2017), but not via direct infusion FTICR-MS. We note that absolute differences in signal
186 intensity may be smaller between molecules at lower concentrations, but this does not necessarily mean that low
187 intensity signals consistently indicate low concentrations and this does not aid in quantitatively interpreting higher
188 intensity signals. In summary, differences in peak intensities across organic compounds do not necessarily equate to
189 differences in concentration, unless assessed via a calibration curve for each compound.

190 3.2 Comparison of peak intensities in in real world samples

191 Routine NOM samples contain a diverse range of thousands of molecules of unknown structures and relative
192 concentrations and often contain inorganic interferences, such as salts. Sample clean up that focuses on pre-
193 concentration and desalting is imperfect (Raeke et al., 2016; Li et al., 2017; Li et al., 2017; Raeke et al., 2016), but
194 is commonly used to minimize inorganic interferences. Interactions among molecules remains a challenge, however,
195 as discussed above. The collection of molecules in a sample is referred to here as the 'matrix.' To explore matrix
196 effects on peak intensities, we prepared solutions of six different pure compounds at a fixed concentration (100 ppb)
197 in three different solvent systems - pure methanol, methanol eluted from a BondElut SPE cartridge, and methanol
198 from elution off of a BondElut SPE cartridge which had been loaded with artificial river water (ARW). Additionally,
199 we added a complex mixture that is often used as a NOM standard, Suwannee River Fulvic Acid (SRFA), at six
200 different concentrations, to each sample. Samples were analyzed independently but contemporaneously on the same
201 instrument to mirror a real study.

202
203 In methanol-only solvent, with no added SRFA, the six compounds yielded different peak intensities (Fig. 4C),
204 which is consistent with results from the previous subsection. As the concentration of SRFA was increased to 2
205 ppm, the relative signal intensity increased for some of the six compounds, but decreased for others. Above 2 ppm
206 of SRFA, peak intensities for all six compounds were substantially decreased. Use of an 'impure' methanol solvent,
207 i.e., the eluent from a SPE blank (Fig. 4D) or from an SPE of artificial river water (Fig. 4E), resulted in further
208 decreases in peak intensities. In both cases, the maximum peak intensity was ~20% of what was seen in pure
209 methanol (Fig. 4C), and some of the six compounds were no longer observed. Addition of SRFA to these samples
210 with 'impure' solvents, again, generally, decreased peak intensities. A 'real-world' sample set would have even
211 greater diversity and heterogeneity than presented here, and thus the issues with use of peak intensities for
212 quantitative interpretation would likely be exacerbated.

213
214 Combining the empirical results from this subsection and the previous subsection with instrument theory discussed
215 above suggests significant uncertainty in relationships between true concentrations and peak intensities from direct
216 infusion FTICR-MS. Calibration curves can be used in the simplest of situations, but ~~may will~~ be challenging when
217 there are unknown variations in structural isomers/isomer and sample-to-sample variation in matrix
218 composition/compositions. Modeling of constrained systems may, however, allow for data-driven and mechanistic
219 data normalization strategies for enhanced use of peak intensity data.

220 3.3 Data Normalization Strategies

221 In the previous section, we use the peak intensities for each analyte without any normalization, only scaling to the
222 base peak or between spectra to make comparison easier. However, more sophisticated or comprehensive
223 normalization strategies may be useful when trying to make quantitative inferences of the data. Considerations may
224 include whether to use the total intensity within a spectrum (including noise, isotopologues, and unannotated
225 features), or to use just the peak intensity apportioned to annotated features. Additionally, non-linear or more

sophisticated functions may have benefits. Such post-hoc statistical approaches have utility for some applications but do not resolve the fundamental, underlying physical origins of the weak connection between peak intensities and true concentrations. We refer readers to the work of Thompson et al. (2021) for more insights into the theory and application of normalization of FTMS for complex mixtures.

4 Conceptual implications for use of ecological metrics

The preceding sections indicate challenges when using FTMS peak intensities as proxies for relative changes in concentrations of organic molecules. The implication is that some ecologically-inspired analyses (e.g., Fig. 1) may be challenging to use with FTMS peak intensity data. To understand which analyses could be impacted, we differentiate analyses into two classes: those based on within-peak intensity comparisons and those based on between-peak intensity comparisons (Fig. 2). As noted above, within-peak is based on comparing the same feature (m/z or molecular formula) across spectra/samples, whereas between-peak compares different features (m/z or molecular formulas) across and within spectra/samples.

We posit that analyses using FTMS between-peak intensity comparisons could have the greatest uncertainty. Consider an ecological setting in which a researcher aims to quantify within-sample diversity (α -diversity) and among-sample diversity (β -diversity) (Fig. 1) of tree communities (Fig. 5, left side). The researcher will likely set up a plot of a given size and then directly count the number of each tree species in each plot, thus generating the species-by-site matrix filled with directly observed abundance counts for each species. The ability of the researcher to observe individuals of each species does not vary appreciably across species because each tree is not moving and our ability to see a static object is not influenced by environmental factors. Thus, the number of individuals observed for a given tree species is quantitatively comparable to the number of individuals observed for all other tree species in the plot. The assumption that differences in observed abundances carry robust information about differences in actual abundances is thus supported, in this example. In turn, it is valid to use relative abundances to compute α -diversity such as via Shannon evenness (Elliott et al., 1997; Mouillot and Leprêtre, 1999; Redowan, 2015); (Elliott et al., 1997; Mouillot and Leprêtre, 1999; Redowan, 2015). Furthermore, because the ability to observe each tree species is the same across communities, it is valid to use relative abundances to compute β -diversity (e.g., via Bray-Curtis; Anderson et al., 2011) (e.g., via Bray-Curtis; Anderson et al., 2011) or conduct other ecological analyses that use abundance data (e.g., species abundance distributions McGill et al., 2007); (e.g., species abundance distributions McGill et al., 2007).

We contrast this tree community example with another ecological setting. Consider a researcher studying bird communities (Fig. 5, right side) that estimated species abundances solely based on the number of times an observer hears the call of a given species. In this case, those species that call more frequently and/or more loudly will be more likely to be heard, and thus an observer will infer a higher abundance even if all species in the community have the same abundance. That is, such a method generates data that may indicate which species are present, but the 'call counts' do not carry reliable information regarding absolute or between-species relative abundances. Follow-on analyses of α -diversity and β -diversity should, therefore, be limited to approaches that use presence/absence data, and species abundance distributions cannot be quantified.

If we continue with the bird community example and assume that the detectability of a given bird species is consistent across sampled locations or times, then it would be appropriate to examine variation in within-species call counts. This within-species analysis is directly analogous to the FTMS within-peak time series analysis in Merder et al. (2021), (2021), discussed below. However, if call counts of a given species are suppressed by the presence or abundance of other species, then call counts of a given species may not indicate changes in its abundance. The call count example is directly analogous to influences of the NOM matrix: if the presence/abundance of a given organic molecule modifies the ionization of other molecules, then within-peak changes in intensity may not indicate changes

274 in concentration. In turn, analyses based on within-peak intensity comparisons could lead to error and uncertainty in
275 values of computed ecological metrics, especially if there are significant cross-sample changes in the NOM matrix.

276
277 As described in the previous sections, the unique chemistry of every molecule in a NOM sample can influence
278 ionization properties for other molecules in the sample. Thus, FTMS data align with the bird community example
279 rather than the tree community example, with the differing physics of each molecule influencing between-peak
280 differences in peak intensity. Molecules that more readily ionize will produce higher peak intensities, which is akin
281 to bird species with noisier or more numerous calls producing a larger number of call counts that do not accurately
282 represent the underlying population distribution. Similarly, between-peak differences in intensity as observed via
283 FTMS cannot be directly used as a proxy to indicate between-peak differences in concentration.

284
285 In contrast to between-peak comparisons, within-peak comparisons examine changes in the relative intensity of a
286 single peak across samples. Such within-peak comparisons may be repeated independently for each peak of interest
287 in a given dataset. For example, Merder et al. (2021)(2021) quantified temporal dynamics of individual FTMS peaks
288 and then binned peaks into different groups with characteristic temporal fluctuations. In those analyses, peak
289 intensities were not compared between peaks. Instead, the temporal dynamics of each peak was compared to
290 temporal dynamics of other peaks. The underlying assumption of this type of analysis is that a between-sample
291 increase in the intensity of a given peak can be used as a robust proxy of a between-sample increase in concentration
292 of that peak. Materials presented in the previous sections indicate that this assumption can be met in some instances
293 when using FTMS data. However, great care is required with strong attention paid to assumptions of analysis
294 methods. For example, using Pearson correlation makes the assumption that concentration of a given peak is a *linear*
295 function of changes in its peak intensity. We showed above (Fig. 4) that this assumption is not always valid, even in
296 ideal conditions. Using a Spearman correlation avoids this assumption because it is based on ranks. That is,
297 Spearman correlations (e.g., Kellerman et al., 2014)(e.g., Kellerman et al., 2014) make the more realistic assumption
298 (for FTMS data) that an increase in concentration of a given peak is reflected as an increase in its peak intensity
299 without assuming any statistical or mathematical form of that relationship.

301 5 Ecological metrics using peak intensities are often robust

302
303 ~~The previous sections highlight challenges in connecting between-peak changes in peak intensity to between-peak~~
304 ~~changes in abundance (Fig. 4). These challenges violate an assumption of abundance-based ecological analyses:~~
305 ~~proxies for abundance (e.g., peak intensity) should be proportional to true abundances. However, the quantitative~~
306 ~~impacts of this situation likely vary across ecological metrics and with study details. There may be certain metrics or~~
307 ~~situations in which robust inferences can be made despite poor linkages between peak intensities and true~~
308 ~~abundances. These cases are important to understand, especially given the growing number of publications using~~
309 ~~peak intensities to compute abundance-based ecological metrics.~~

310
311 The previous sections highlight challenges in connecting between-peak changes in observed intensity to between-
312 peak changes in true abundance (Fig. 4). These challenges violate an assumption of abundance-based ecological
313 analyses: proxies for abundance (e.g., peak intensity) should be proportional to true abundances. However, the
314 quantitative impacts of this situation likely vary across ecological metrics and with study details. There may be
315 certain metrics or conditions in which robust inferences can be made despite poor linkages between peak intensities
316 and true abundances. These cases are important to understand for robust use of abundance-based ecological metrics
317 in FTMS NOM studies.

318
319 To provide initial guidance on best practices for using FTMS peak intensities with ecological metrics, we developed
320 an *in silico* simulation model: (full details are in Supplementary Material). This model generates synthetic data, and
321 introduces errors that degrade the linkage between peak intensity and true abundance, and computes within sample

(e.g., Shannon diversity) and between-sample (e.g., Bray-Curtis) ecological metrics (Fig. 7). Simulated values that are influenced by introduced errors are conceptually analogous to intensities from real-world FTMS NOM studies. This allows us to probe how errors inherent to FTMS may impact (6). The model allows us to probe how the introduction of each type of error impacts the relationship between true and observed values of ecological metrics. To generate synthetic data, we randomly assigned abundances to the simulation model produced samples with either 100 or 1000 peaks. Abundances were sampled with replacement from a Gaussian distribution that varied in mean and standard deviation across synthetic samples and across simulation iterations. Abundances were drawn twice to generate. This was done to study how the influences of errors change with the number of peaks; going above 1000 peaks did not change the outcomes and going below 100 peaks is unlikely to be relevant to many FTMS studies. For each run of the model, the true abundances of each peak within each of two independent samples per simulation, and the simulation was run 100 times for each number of peaks (100 or 1000 peaks per sample; referred to below as 'peak richness'). We varied the were randomly assigned from Gaussian distributions to generate synthetic that differed across samples varying in composition within and across simulations to ensure that the ecological metrics (see below) would vary across simulations. This step was necessary to evaluate metric performance across a broad range of metric values.

and simulation iterations. We simulated two types of error which can both be representative of that modified the true abundances; within-sample error reflects variation in ionization efficiency. The goal was to generate synthetic data that mimicked our empirical and theoretical observations that indicate noise in the relationships between observed peak intensities and true abundances. For each type of error and within each iteration of the simulation, the error was introduced 100 times (i.e., 100 error iterations were nested within each sample-generation iteration). The first type of error was designed to diminish the between-peak relationship between observed peak intensity and true abundance. To introduce this error, we multiplied the true abundance of each peak by a random number drawn from a uniform distribution ranging from 0 to 100. The inclusion of 0 indicates situations in which a given peak (i.e., ion) does not ionize well enough to be observed. The results should not be sensitive to the selected range, but as a sensitivity analysis, we also used a distribution of errors ranging from 0 to 8. Our empirical data suggest that this narrower range is appropriate (Fig. 4B), but simulation results were not affected by the selected error range (Supplementary Figs. S3-S8). For each peak we multiplied the same random error by its abundance in each of the two synthetic samples within each iteration. This error modified abundance of each peak in each synthetic sample was considered to be the observed peak intensity. We recognize that randomized errors do not perfectly reflect real-world across molecules (but not across samples) and between-sample error reflects variation in ionization efficiency. However, because the true impacts of matrix effects and individual molecular chemistries in complex mixtures are currently not known, the errors introduced in the model are simply used to diminish the relationship between observed peak intensities and true abundances.

Introducing error resulted in a relatively weak relationship between observed peak intensity and true abundance (median $R^2 = -0.5$; see black line in Figure 7), with the amount of error increasing with true abundance (Fig. across S1). This relationship additionally supports our inclusion of error into the model as a means to simulate relatively weak relationships between observed peak intensity and true abundance. Between-peak differences in observed intensity were also weakly related to between-peak differences in true abundance (Fig. 8A), with a median R^2 of -0.5 (see blue line in Figure 7). Because the same peak-level error factor was used across both synthetic samples within a given simulation iteration, the within-peak between-sample differences in observed intensity were relatively strongly correlated to within-peak between-sample differences in true abundance (Fig. 8C), with a median R^2 of -0.75 (see the gray line in Figure 7). As seen in Figure 8C, the differences collapse when near zero. This phenomenon can be explained by the fact that when two samples have essentially the same peak intensity for a given peak, introducing the same error to that peak in both samples has little influence on the between-sample difference in peak intensity.

The second type of error we introduced represents situations in which ionization efficiency varies across molecules—as in the first type of error—as well as across samples. Molecules may exhibit variations in ionization efficiency across samples due to changes in the composition of organic molecules and/or changes in inorganic solutes in the matrix (see above). To account for these effects, we multiplied the true abundance of each peak by a random number drawn from a uniform distribution ranging from 0 to 100; for sensitivity analysis, we also used an error distribution ranging from 0 to 8, which did not have meaningful influences on the results. For each iteration of the simulation, we introduced errors independently for the two synthetic samples. In this way, the simulated ionization efficiency for a given peak in a given synthetic sample was independent of its ionization efficiency in the other synthetic sample. The error-modified abundance of each peak in each synthetic sample was considered to be the observed peak intensity samples.

We observed a relatively large influence on observed peak intensities when allowing ionization efficiency to vary across samples. That is, the within-peak between-sample differences in observed intensity were weakly correlated to within-peak between-sample differences in true abundance (Fig. 8C), with a median R^2 of -0.5 (see the red line in Figure 7). Compared to the same relationship that emerged under the first type of error, our results show a much weaker relationship between peak intensity and true abundance when ionization efficiency varies between samples (compare the gray and red lines in Figure 7). This result is expected, as variations in ionization efficiency add random noise to the within-peak between-sample differences in observed peak intensity. We note that the variation in ionization efficiency is independent between peaks for both the first and second types of error. The between-peak relationship summarized in Figure 7 (blue line) is, therefore, equivalent for both types of error, which is further supported by the strong similarity between Figures 8A and 8B.

To examine how both types of error influence ecological metrics, we used the initial true abundances and the error-modified abundances (i.e., analogous to observed peak intensity values/intensities) to calculate true and 'observed' values of within-sample α -diversity via the Shannon diversity metric, between-sample β -diversity via the Bray-Curtis metric. We also assigned dissimilarity metric, and a generic intensity-weighted sample-level mean trait value based on assigning an arbitrary trait value to each peak (Fig. 6), and calculated true and observed sample-level mean trait values; the mean values for each sample were weighted by true abundance (true mean) or observed peak intensity (observed mean). This trait analysis is analogous to the approach commonly used in ecological studies for computing community-level abundance-weighted trait values, such as plant leaf area index or animal body size (Muscarella and Uriarte, 2016). This mean trait approach is also commonly used with FTMS data, such as for sample-level peak-intensity-weighted values of hydrogen-to-carbon stoichiometric ratios (e.g., H:C) and several other metrics derived from molecular weight (Roth et al., 2019; Wen et al., 2021). We regressed observed values for Shannon diversity, Bray-Curtis, and mean traits against their true values, and performed this process independently for each level of peak richness/formulae (Roth et al., 2019; Wen et al., 2021).

Relating error-influenced 'observed' values of each ecological metric to their true values revealed that the patterns observed in peak-intensity-based ecological metrics are actually likely to be qualitatively robust despite the existence of quantitative biases (Figs. 7-9-14). All three ecological metrics showed monotonic relationships between observed and true values—for both types of error; in Figures 7-9 all A/C and B/D panels have within-sample and between-sample error, respectively. Uncertainty was lower when samples had 1000 peaks, relative to samples with 100 peaks; in Figures 7-9-14 all A/B and C/D panels have 100 and 1000 peaks, respectively. We observed monotonic relationships and lower uncertainty with more peaks for both within-sample and between-sample error; in Figures 9-11 all A/C and B/D panels have within-sample and between-sample errors, respectively. For Shannon diversity, observed values were consistently lower than true values, but all observed vs. true relationships were linear (Fig. 9Z). For Bray-Curtis, inclusion of between-sample error resulted in an overestimation of values and non-linear (but monotonic) relationships between observed and true values (Fig. 10Z). For mean trait values, we found no systematic quantitative biases, and the relationships between observed and true values were consistently linear (Fig. 11-9).

Formatted: Header

419
420 The variation in observed values explained by true values (via a linear model) increases rapidly with the number of
421 peaks and ~~sharply~~ asymptotes beyond ~500-1000 peaks per sample (Fig. ~~S1, S2~~). ~~Sample~~ The number of peaks
422 needed to reach the asymptote and minimize uncertainty is likely dataset dependent and 500-1000 peaks should not
423 be taken as a general rule for real-world datasets. Nonetheless, we propose that qualitative gradients based on
424 sample-to-sample changes in the value of ecological metrics can, therefore, generally be interpreted with increasing
425 confidence as the number of peaks increases. Qualitative gradients are, therefore, more robust with more peaks. The
426 Quantitative comparisons from one dataset to another may, however, require further simulation-based evaluation as
427 the absolute magnitude of some ecological metrics, however, are shifted away from their true magnitude
428 even when there are large numbers of peaks (e.g., Fig. 8D, 10D). Quantitative comparisons from one dataset to
429 another may, therefore, require further simulation-based evaluation. We further caution that the number of peaks
430 needed to reach the asymptote, thereby minimizing error, is likely dataset dependent, and 500-1000 peaks should not
431 be taken as a general rule for real-world datasets. We encourage researchers to ~~complete such simulations using~~
432 the simulation model with the numbers of peaks present across their own real-world datasets to better understand
433 their ability to make statistical and conceptual inferences.

Formatted: Font: 10 pt

434 6 Conclusions and Recommendations

435 There is ~~increasing interest~~ significant value in using ecological metrics with FTMS data to study NOM chemistry -
436 ~~It~~ (Bahureksa et al., 2021; Cooper et al., 2022; Spencer et al., 2015; Stubbins et al., 2010), and it is vital that this
437 ~~growing body of work be done~~ based on rigorous use of the data. ~~This requires deep understanding of the metrics,~~
438 ~~awareness of the~~ When using ecological metrics with FTMS NOM data it is important to understand how the
439 assumptions and limitations, and careful use of the metrics informed by the data relate to limitations of the data. We
440 suggest that studies using FTMS peak intensities need to include material that directly discusses the data limitations,
441 what peak intensities do and do not represent (e.g., tree-like vs. bird-like data; Fig. 5), and how knowledge of those
442 limitations was used to select specific metrics.

443
444 We have provided both theoretical reasoning and empirical observations showing that peak intensities do not
445 necessarily map to concentrations of the associated organic molecules within NOM-like complex mixtures of
446 organic molecules. This is particularly true for between-peak comparisons, and statistical post-hoc normalizations of
447 peak intensity data do not solve this challenge. We caution against using between-peak differences in intensity from
448 FTMS data to make direct inferences related to between-peak differences in abundance or concentration. This has
449 implications for some ecological analyses based directly on variation in species abundances. ~~In particular, such as,~~
450 For example, estimation of 'species abundance distributions' are likely to be problematic. Analyses that bin peaks
451 into high and low abundance groups based on between-peak differences in concentration are also likely to be
452 problematic. We did not directly evaluate these types of analyses, and we suggest that future work should expand
453 upon the ecological metrics examined here via simulation.

454
455 While there are challenges and limitations in the use of ecological metrics with FTMS data, we show that there is a
456 tangible path forward. In particular, our simulation model revealed good performance of some common ecological
457 metrics of α -diversity, β -diversity, and functional mean trait values. We infer that conceptual and mechanistic
458 inferences are likely to be valid when based on analyses such as comparing peak-intensity-based ecological metrics
459 across experimental treatments or variation along environmental gradients. The performance of intensity-weighted
460 mean trait values was particularly good ~~in terms of,~~ both qualitatively and quantitatively. This indicates
461 that using peak intensities to estimate sample-level mean traits/properties likely provides quantitatively robust
462 estimates, such as for stoichiometric ratios (e.g., H/C, O/C) and many other commonly calculated quantitative
463 aspects. We emphasize that properties related to molecular formulas (e.g., nominal oxidation state of carbon,
464 aromaticity index, double bond equivalent, etc.).

466 As general guidance we studied a small setsuggest avoiding analyses that make direct use of between-peak
467 comparisons of peak intensity and rely instead on derived metrics and our inferences only extend to these that use
468 intensities from large numbers of peaks. For example, while peak-intensity-weighted mean trait values appear to be
469 robust, our physical experiments indicate caution against direct comparison of peak intensities to infer between-peak
470 differences in concentration. This is relevant to analyses such as comparing peak intensities within a Van-Krevelen
471 analysis or across classes of elemental composition (e.g., CHO, CHON, etc.). Such analyses could be problematic as
472 quantitative variation in peak intensities across the Van-Krevelen space or across classes of elemental composition is
473 likely influenced by variation in ionization efficiencies with unclear connections to true concentrations. It is,
474 therefore, not recommended to use peak intensities to identify parts of Van-Krevelen space (e.g., protein-like
475 compounds) or compositional classes that have the highest concentrations in a given sample. It is preferable to
476 report the fractions of peaks contained within different parts of Van-Krevelen space or within different
477 compositional classes and avoid quantitative estimates based on peak intensities (e.g., percent of total sample-level
478 intensity found within a given class). An alternative approach for robust and direct use of peak intensities, based on
479 our physical experiments, is the use of Spearman-based correlations for within-peak comparisons across samples.
480 Such correlations could be done across spatial environmental gradients, through time, and/or with respect to other
481 sample-level quantitative measurements (e.g., organic carbon concentration). This implies that other types of
482 correlation-based analyses are likely robust, such as peak intensity-based network analyses. We further suggest that
483 parametric statistics can often be used to relate the ecological metrics- studied here to other quantitative variables,
484 both directly (e.g., via Pearson-based correlation) and indirectly (e.g., via Bray-Curtis based non-metric
485 multidimensional scaling).

486
487 There are many other kinds of analyses currently done with FTMS data and more will be imagined in the future. To
488 develop further guidance on how to best use peak intensities for a broader range of analyses we recommend use and
489 further development of the simulation model developed here. Fortunately, it is straightforward to extend the
490 simulation model to additional metrics (e.g., Hill numbers; Hill, 1973) and analyses (e.g., species abundance
491 distributions; McGill et al., 2007)-(e.g., Hill numbers; Hill, 1973) and analyses (e.g., species abundance
492 distributions; McGill et al., 2007). We suggest that users of FTMS data do this before applying abundance-based
493 ecological metrics to real-world datasets. This will provide objective guidance on how to use (and whether to avoid)
494 specific metrics for specific FTMS datasets.

495
496 To enable robust use of FTMS peak intensity data in future studies, we recommend use and further development of
497 the simulation model developed here. The simulation model is the only tool we are aware of that can provide
498 objective evaluations of uncertainty and potential biases associated with using FTMS peak intensities to compute
499 ecological metrics. The model should not be taken as a static or mature tool, however. We encourage future work to
500 expand it to include additional ecological metrics/analyses, situations with more than two samples, sample-to-
501 sample variation in peak richness, links between peak richness and peak intensity, other ways of modeling
502 error-explicit molecular properties/traits, non-random errors, and measured levels of error between concentrations
503 and peak intensities. TheseIt can be further extended to directly add error into peak intensities from real-world
504 FTMS data and re-calculate ecological metrics of interest across a range of introduced error. This would help gauge
505 the robustness of conceptual inferences derived from peak intensity-based analyses.

506
507 Further evaluations are outside of the scope of this work, but will be straightforward to include in future versions of
508 the simulation model. ~~Such additions will allow~~ We envision each study ~~to customize~~ customizing the model for their
509 specific application. ~~It should~~ For any real-world study, the model can be ~~possible~~ modified to include the actual
510 number of samples, the number of peaks in each sample, the peak intensity distributions, number of replicates, and
511 the specific ecological analyses that will be applied. In turn, simulation model outcomes can provide objective
512 guidance tailored to each study. One may think of the resulting guidance as akin to a power analysis whereby the
513 simulation can indicate what can and cannot be inferred from a given dataset. For example, the model indicates that
514 observed Bray-Curtis values have little to no correspondence to true values when Bray-Curtis is below ~0.2 (Fig.

Formatted: Header

515 40B8B, D). Bray-Curtis near and below ~0.2 are commonly observed in FTMS studies (e.g., Hawkes et al., 2016;
516 Derrien et al., 2018; Bao et al., 2018); (Bao et al., 2018; Derrien et al., 2018; e.g., Hawkes et al., 2016), and this
517 disconnect between observations and truth is maintained even with 1000 peaks per sample (Fig. 40D8D). In turn,
518 FTMS studies that observe Bray-Curtis below ~0.2 may not be able to use those observations to make valid
519 conceptual inferences. However, quantitative guidance must be developed for each study and we recommend that a
520 version of the simulation model should be used by future studies using peak intensities to conduct ecological
521 analyses of FTMS data. It may be that in time we understand the general rules well enough to leave the simulation
522 behind, but for now, we suggest its use is warranted to ensure robust inferences.

523
524 In addition to further use and development of the simulation model, we recommend translation of other modeling
525 approaches for use with FTMS data. Two potential approaches are based in machine learning and hierarchical
526 modeling. Machine learning could be used to model the instrument response for a diverse chemical space in typical
527 environmental samples to learn how measured signal intensities may relate to true concentrations. Even if such a
528 model does not yield high-accuracy results, it may nonetheless help understand error/biases and provide additional
529 guidance for robust use of peak intensity data. Potentially in concert with machine learning, hierarchical modeling
530 could be translated from its application in ecological analyses (Iknavan et al., 2014) (Iknavan et al., 2014) for use
531 with FTMS. This approach has been used to model sources of error that lead to variation in detectability across
532 biological species, such as variation in species visibility (e.g., Dorazio and Royle, 2005); (e.g., Dorazio and Royle,
533 2005). In turn, data can essentially be corrected by accounting for the modeled sources of error (Roth et al.,
534 2018); (Roth et al., 2018), even revealing 'hidden diversity' (Richter et al., 2021); (Richter et al., 2021). There are
535 likely direct analogs to FTMS data in terms of variation among molecules in detectability due to variation in
536 ionization and molecular interactions discussed in previous sections. Machine learning could be used to understand
537 sources of error and, in turn, inform hierarchical models aimed at improving the mapping between peak intensity
538 and concentration. If successful, this would increase the quality of information provided by peak intensities in both
539 existing and future datasets.

540
541 In summary, FTMS has many strengths and weaknesses just like any analytical platform. Other types of
542 compositional data also contain biases and uncertainties, such as the lack of true quantitation in sequence-based
543 microbiome data (Gloor et al., 2017); (Gloor et al., 2017). Careful use of FTMS peak intensity data informed by
544 objective, model-based guidance can overcome some of its weaknesses. We encourage further development of the
545 model presented here and inclusion of additional methods developed to address issues that arise in similar data types
546 (e.g., Gloor et al., 2017; Hardwick et al., 2018; Vieira-Silva et al., 2019); (e.g., Gloor et al., 2017; Hardwick et al.,
547 2018; Vieira-Silva et al., 2019). While these are important directions, we emphasize that despite peak intensities not
548 necessarily reflecting concentrations, ecological metrics overall appear to perform well. This is likely due to the law
549 of large numbers as FTMS, especially FTICR MS, datasets often contain 1000 or more peaks per sample. Our
550 simulation results indicate that large numbers of identified peaks allow ecological metrics to essentially track
551 towards their true values. We are encouraged by this outcome and look forward to further applications of ecological
552 metrics, concepts, and theory to NOM chemistry. Such advances could be greatly facilitated by a public database of
553 standardized FTICR MS datasets paired with push-button execution of the simulation model for user-defined
554 metrics and subsets of the database.

555
556 **7 Code Availability:** R code for running the simulation models is available on GitHub:

557 https://github.com/stegen/Peak_Intensity_Sims. Python code used to process the empirical data and to generate the
558 associated figures will be available upon publication.

559
560 **8 Data Availability:** Raw and processed data will be made publicly available upon manuscript acceptance.

Formatted: Normal

Formatted: Normal

Formatted: Header

Formatted: Normal

562 **9 Author Contributions:** WK contributed to conceptualization, experimental data curation, formal analysis,
563 methodology, software, visualization, writing-original draft, writing-review/editing; AMP contributed to
564 conceptualization, methodology, visualization, writing-original draft, writing-review/editing; CHC and SMC
565 contributed to investigation and writing-review/editing; JE contributed to sample preparation and writing-
566 review/editing; MMT contributed to conceptualization, methodology, writing-review/editing; JH contributed to
567 conceptualization and writing-review/editing; RKC contributed to project administration, conceptualization,
568 experimental data curation, methodology, [funding acquisition](#), writing-review/editing; JCS contributed to
569 conceptualization, simulation data curation, formal analysis, funding acquisition, investigation, methodology,
570 software, visualization, writing-original draft, writing-review/editing.

571 **10 Competing interests:** The authors declare that they have no conflict of interest.

572
573 **11 Acknowledgements:** A portion of this research was performed on a project award
574 (doi:10.46936/intm.proj.2020.51667/60000248) from the Environmental Molecular Sciences Laboratory, a DOE
575 Office of Science User Facility sponsored by the Biological and Environmental Research program under Contract
576 No. DE-AC05-76RL01830. JCS was also supported by an Early Career Award (grant 74193) to JCS at Pacific
577 Northwest National Laboratory (PNNL), a multiprogram national laboratory operated by Battelle for the United
578 States Department of Energy under contract DE-AC05-76RL01830. We thank Alan Roebuck for useful feedback on
579 the manuscript, Nathan Johnson for graphics development, Charles T. Resch for supplying the artificial river water,
580 Patricia Miller and Jason Toyoda for lab support.

581 12 References

- 582 Anderson, M. J., Crist, T. O., Chase, J. M., Vellend, M., Inouye, B. D., Freestone, A. L., Sanders, N. J.,
583 Cornell, H. V., Comita, L. S., Davies, K. F., Harrison, S. P., Kraft, N. J. B., Stegen, J. C., and
584 Swenson, N. G.: Navigating the multiple meanings of β diversity: a roadmap for the practicing
585 ecologist, *Ecol. Lett.*, 14, 19–28, <https://doi.org/10.1111/j.1461-0248.2010.01552.x>, 2011.
- 586 Bahureksa, W., Tfaily, M. M., Boiteau, R. M., Young, R. B., Logan, M. N., McKenna, A. M., and Boreh,
587 T.: Soil Organic Matter Characterization by Fourier Transform Ion Cyclotron Resonance Mass
588 Spectrometry (FTICR MS): A Critical Review of Sample Preparation, Analysis, and Data
589 Interpretation, *Environ. Sci. Technol.*, 55, 9637–9656, <https://doi.org/10.1021/acs.est.1c01135>, 2021.
- 590 Bao, H., Niggemann, J., Luo, L., Dittmar, T., and Kao, S. J.: Molecular composition and origin of water-
591 soluble organic matter in marine aerosols in the Pacific off China, *Atmos. Environ.*, 191, 27–35,
592 <https://doi.org/10.1016/j.atmosenv.2018.07.059>, 2018.
- 593 Boye, K., Noël, V., Tfaily, M. M., Bone, S. E., Williams, K. H., Bargar, J. R., and Fendorf, S.:
594 Thermodynamically controlled preservation of organic carbon in floodplains, *Nat. Geosci.*, 10, 415–
595 419, <https://doi.org/10.1038/ngeo2940>, 2017.
- 596 Cao, D., Lv, J., Geng, F., Rao, Z., Niu, H., Shi, Y., Cai, Y., and Kang, Y.: Ion Accumulation Time
597 Dependent Molecular Characterization of Natural Organic Matter Using Electrospray Ionization-
598 Fourier Transform Ion Cyclotron Resonance Mass Spectrometry, *Anal. Chem.*, 88, 12210–12218,
599 <https://doi.org/10.1021/acs.analchem.6b03198>, 2016.
- 600 Danczak, R. E., Chu, R. K., Fansler, S. J., Goldman, A. E., Graham, E. B., Tfaily, M. M., Toyoda, J., and
601 Stegen, J. C.: Using metacommunity ecology to understand environmental metabolomes, *Nat.*
602 *Commun.*, 11, 6369, <https://doi.org/10.1038/s41467-020-19989-y>, 2020.
- 603 Danczak, R. E., Goldman, A. E., Chu, R. K., Toyoda, J. G., Garayburu-Caruso, V. A., Tolić, N., Graham,
604 E. B., Morad, J. W., Renteria, L., Wells, J. R., Herzog, S. P., Ward, A. S., and Stegen, J. C.:
605 Ecological theory applied to environmental metabolomes reveals compositional divergence despite
606 conserved molecular properties, *Sci. Total Environ.*, 788, 147409,
607 <https://doi.org/10.1016/j.scitotenv.2021.147409>, 2021.
- 608 Derrien, M., Lee, Y. K., Shin, K. H., and Hur, J.: Comparing discrimination capabilities of fluorescence

609 spectroscopy versus FT-ICR-MS for sources and hydrophobicity of sediment organic matter, *Environ-*
610 *Sci. Pollut. Res.*, 25, 1892–1902, <https://doi.org/10.1007/s11356-017-0531-z>, 2018.

611 Dorazio, R. M. and Royle, J. A.: Estimating Size and Composition of Biological Communities by
612 Modeling the Occurrence of Species, *J. Am. Stat. Assoc.*, 100, 389–398,
613 <https://doi.org/10.1198/016214505000000015>, 2005.

614 Elliott, K. J., Boring, L. R., Swank, W. T., and Haines, B. R.: Successional changes in plant species
615 diversity and composition after clearcutting a Southern Appalachian watershed, *For. Ecol. Manag.*,
616 92, 67–85, [https://doi.org/10.1016/S0378-1127\(96\)03947-3](https://doi.org/10.1016/S0378-1127(96)03947-3), 1997.

617 Garayburu-Caruso, V. A., Stegen, J. C., Song, H. S., Renteria, L., Wells, J., Garcia, W., Resch, C. T.,
618 Goldman, A. E., Chu, R. K., Toyoda, J., and Graham, E. B.: Carbon Limitation Leads to
619 Thermodynamic Regulation of Aerobic Metabolism, *Environ. Sci. Technol. Lett.*, 7, 517–524,
620 <https://doi.org/10.1021/acs.estlett.0e00258>, 2020.

621 Gloor, G. B., Macklaim, J. M., Pawlowsky-Glahn, V., and Egozeu, J. J.: Microbiome Datasets Are
622 Compositional: And This Is Not Optional, *Front. Microbiol.*, 8, 2017.

623 Han, L., Kaesler, J., Peng, C., Reemtsma, T., and Lechtenfeld, O. J.: Online Counter Gradient LC-FT-
624 ICR-MS Enables Detection of Highly Polar Natural Organic Matter Fractions, *Anal. Chem.*, 93,
625 1740–1748, <https://doi.org/10.1021/acs.analchem.0e04426>, 2021.

626 Hardwick, S. A., Chen, W. Y., Wong, T., Kanakamedala, B. S., Deveson, I. W., Ongley, S. E., Santini, N.
627 S., Marcellin, E., Smith, M. A., Nielsen, L. K., Lovelock, C. E., Neilan, B. A., and Mercer, T. R.:
628 Synthetic microbe communities provide internal reference standards for metagenome sequencing and
629 analysis, *Nat. Commun.*, 9, 3096, <https://doi.org/10.1038/s41467-018-05555-0>, 2018.

630 Hawkes, J. A. and Kew, W.: 4 High resolution mass spectrometry strategies for the investigation of
631 dissolved organic matter, in: *Multidimensional Analytical Techniques in Environmental Research*,
632 edited by: Duarte, R. M. B. O. and Duarte, A. C., Elsevier, 71–104, [https://doi.org/10.1016/B978-0-](https://doi.org/10.1016/B978-0-12-818896-5.00004-1)
633 [12-818896-5.00004-1](https://doi.org/10.1016/B978-0-12-818896-5.00004-1), 2020a.

634 Hawkes, J. A. and Kew, W.: 4 High resolution mass spectrometry strategies for the investigation of
635 dissolved organic matter, in: *Multidimensional Analytical Techniques in Environmental Research*,
636 edited by: Duarte, R. M. B. O. and Duarte, A. C., Elsevier, 71–104, [https://doi.org/10.1016/B978-0-](https://doi.org/10.1016/B978-0-12-818896-5.00004-1)
637 [12-818896-5.00004-1](https://doi.org/10.1016/B978-0-12-818896-5.00004-1), 2020b.

638 Hawkes, J. A., Dittmar, T., Patriarea, C., Tranvik, L., and Bergquist, J.: Evaluation of the Orbitrap Mass
639 Spectrometer for the Molecular Fingerprinting Analysis of Natural Dissolved Organic Matter, *Anal.*
640 *Chem.*, 88, 7698–7704, <https://doi.org/10.1021/acs.analchem.6b01624>, 2016.

641 Hedges, J. I., Eglinton, G., Hatcher, P. G., Kirchman, D. L., Arnosti, C., Derenne, S., Evershed, R. P.,
642 Kögel-Knabner, I., de Leeuw, J. W., Littke, R., Michaelis, W., and Rullkötter, J.: The molecularly-
643 uncharacterized component of nonliving organic matter in natural environments, *Org. Geochem.*, 31,
644 945–958, [https://doi.org/10.1016/S0146-6380\(00\)00096-6](https://doi.org/10.1016/S0146-6380(00)00096-6), 2000.

645 Hill, M. O.: Diversity and Evenness: A Unifying Notation and Its Consequences, *Ecology*, 54, 427–432,
646 <https://doi.org/10.2307/1934352>, 1973.

647 Hknayan, K. J., Tingley, M. W., Furnas, B. J., and Beissinger, S. R.: Detecting diversity: emerging
648 methods to estimate species diversity, *Trends Ecol. Evol.*, 29, 97–106,
649 <https://doi.org/10.1016/j.tree.2013.10.012>, 2014.

650 Kaiser, N. K., McKenna, A. M., Savory, J. J., Hendrickson, C. L., and Marshall, A. G.: Tailored Ion
651 Radius Distribution for Increased Dynamic Range in FT-ICR Mass Analysis of Complex Mixtures,
652 *Anal. Chem.*, 85, 265–272, <https://doi.org/10.1021/ac302678v>, 2013.

653 Kellerman, A. M., Dittmar, T., Kothawala, D. N., and Tranvik, L. J.: Chemodiversity of dissolved organic
654 matter in lakes driven by climate and hydrology, *Nat. Commun.*, 5, 3804,
655 <https://doi.org/10.1038/ncomms4804>, 2014.

656 Kim, D., Kim, S., Son, S., Jung, M. J., and Kim, S.: Application of Online Liquid Chromatography-7 T
657 FT-ICR Mass Spectrometer Equipped with Quadrupolar Detection for Analysis of Natural Organic
658 Matter, *Anal. Chem.*, 91, 7690–7697, <https://doi.org/10.1021/acs.analchem.9b00689>, 2019.

659 Krueve, A.: Strategies for Drawing Quantitative Conclusions from Nontargeted Liquid Chromatography-

- 660 High-Resolution Mass Spectrometry Analysis, *Anal. Chem.*, 92, 4691–4699,
661 <https://doi.org/10.1021/acs.analchem.9b03481>, 2020.
- 662 Krueve, A., Kaupmees, K., Liigand, J., and Leito, I.: Negative Electrospray Ionization via Deprotonation:
663 Predicting the Ionization Efficiency, *Anal. Chem.*, 86, 4822–4830,
664 <https://doi.org/10.1021/ac404066v>, 2014.
- 665 Kujawinski, E. B.: Electrospray Ionization Fourier Transform Ion Cyclotron Resonance Mass
666 Spectrometry (ESI FT ICR MS): Characterization of Complex Environmental Mixtures, *Environ.*
667 *Forensics*, 3, 207–216, <https://doi.org/10.1006/enfo.2002.0109>, 2002.
- 668 Kujawinski, E. B., Longnecker, K., Blough, N. V., Vecchio, R. D., Finlay, L., Kitner, J. B., and
669 Giovannoni, S. J.: Identification of possible source markers in marine dissolved organic matter using
670 ultrahigh-resolution mass spectrometry, *Geochim. Cosmochim. Acta*, 73, 4384–4399,
671 <https://doi.org/10.1016/j.gca.2009.04.033>, 2009.
- 672 LaRowe, D. E. and Van Cappellen, P.: Degradation of natural organic matter: A thermodynamic analysis,
673 *Geochim. Cosmochim. Acta*, 75, 2030–2042, <https://doi.org/10.1016/j.gca.2011.01.020>, 2011.
- 674 Leyva, D., Tose, L. V., Porter, J., Wolff, J., Jaffé, R., and Fernandez-Lima, F.: Understanding the
675 structural complexity of dissolved organic matter: isomeric diversity, *Faraday Discuss.*, 218, 431–
676 440, <https://doi.org/10.1039/C8FD00221E>, 2019.
- 677 Leyva, D., Jaffe, R., and Fernandez-Lima, F.: Structural Characterization of Dissolved Organic Matter at
678 the Chemical Formula Level Using TIMS FT ICR MS/MS, *Anal. Chem.*, 92, 11960–11966,
679 <https://doi.org/10.1021/acs.analchem.0c02347>, 2020.
- 680 Li, H. Y., Wang, H., Wang, H. T., Xin, P. Y., Xu, X. H., Ma, Y., Liu, W. P., Teng, C. Y., Jiang, C. L.,
681 Lou, L. P., Arnold, W., Cralle, L., Zhu, Y. G., Chu, J. F., Gilbert, J. A., and Zhang, Z. J.: The
682 chemodiversity of paddy soil dissolved organic matter correlates with microbial community at
683 continental scales, *Microbiome*, 6, 187, <https://doi.org/10.1186/s40168-018-0561-x>, 2018.
- 684 Li, Y., Harir, M., Uhl, J., Kanawati, B., Lucio, M., Smirnov, K. S., Koch, B. P., Schmitt-Kopplin, P., and
685 Hertkorn, N.: How representative are dissolved organic matter (DOM) extracts? A comprehensive
686 study of sorbent selectivity for DOM isolation, *Water Res.*, 116, 316–323,
687 <https://doi.org/10.1016/j.watres.2017.03.038>, 2017.
- 688 Lucas, J., Koester, I., Wichels, A., Niggemann, J., Dittmar, T., Callies, U., Wiltshire, K. H., and Gerds,
689 G.: Short-Term Dynamics of North Sea Bacterioplankton Dissolved Organic Matter Coherence on
690 Molecular Level, *Front. Microbiol.*, 7, 2016.
- 691 Makarov, A., Denisov, E., Kholomeev, A., Balsehun, W., Lange, O., Strupat, K., and Horning, S.:
692 Performance Evaluation of a Hybrid Linear Ion Trap/Orbitrap Mass Spectrometer, *Anal. Chem.*, 78,
693 2113–2120, <https://doi.org/10.1021/acs.0518811>, 2006.
- 694 Makarov, A., Grinfeld, D., and Ayzikov, K.: Chapter 2 – Fundamentals of Orbitrap analyzer, in:
695 Fundamentals and Applications of Fourier Transform Mass Spectrometry, edited by: Kanawati, B.
696 and Schmitt-Kopplin, P., Elsevier, 37–61, <https://doi.org/10.1016/B978-0-12-814013-0.00002-8>,
697 2019.
- 698 Marshall, A. G., Hendrickson, C. L., and Jackson, G. S.: Fourier transform ion cyclotron resonance mass
699 spectrometry: A primer, *Mass Spectrom. Rev.*, 17, 1–35, [https://doi.org/10.1002/\(SICI\)1098-2787\(1998\)17:1<1::AID-MAS1>3.0.CO;2-K](https://doi.org/10.1002/(SICI)1098-2787(1998)17:1<1::AID-MAS1>3.0.CO;2-K), 1998.
- 700 McGill, B. J., Etienne, R. S., Gray, J. S., Alonso, D., Anderson, M. J., Benceha, H. K., Dornelas, M.,
701 Enquist, B. J., Green, J. L., He, F., Hurlbert, A. H., Magurran, A. E., Marquet, P. A., Maurer, B. A.,
702 Ostling, A., Soykan, C. U., Ugland, K. I., and White, E. P.: Species abundance distributions: moving
703 beyond single-prediction theories to integration within an ecological framework, *Ecol. Lett.*, 10, 995–
704 1015, <https://doi.org/10.1111/j.1461-0248.2007.01094.x>, 2007.
- 705 Merder, J., Röder, H., Dittmar, T., Feudel, U., Freund, J. A., Gerds, G., Kraberg, A., and Niggemann, J.:
706 Dissolved organic compounds with synchronous dynamics share chemical properties and origin,
707 *Limnol. Oceanogr.*, n/a, <https://doi.org/10.1002/lno.11938>, 2021.
- 708 Mouillot, D. and Lepêtre, A.: A comparison of species diversity estimators, *Res. Popul. Ecol.*, 41, 203–
709 215, <https://doi.org/10.1007/s101440050024>, 1999.

- 711 Muscarella, R. and Uriarte, M.: Do community-weighted mean functional traits reflect optimal
712 strategies?, *Proc. R. Soc. B Biol. Sci.*, 283, 20152434, <https://doi.org/10.1098/rspb.2015.2434>, 2016.
- 713 Osterholz, H., Singer, G., Wemheuer, B., Daniel, R., Simon, M., Niggemann, J., and Dittmar, T.:
714 Deciphering associations between dissolved organic molecules and bacterial communities in a pelagic
715 marine system, *ISME J.*, 10, 1717–1730, <https://doi.org/10.1038/ismej.2015.231>, 2016.
- 716 Raake, J., Lechtenfeld, O. J., Wagner, M., Herzsprung, P., and Reemtsma, T.: Selectivity of solid phase
717 extraction of freshwater dissolved organic matter and its effect on ultrahigh resolution mass spectra,
718 *Environ. Sci. Process. Impacts*, 18, 918–927, <https://doi.org/10.1039/C6EM00200E>, 2016.
- 719 Redowan, M.: Spatial pattern of tree diversity and evenness across forest types in Majella National Park,
720 Italy, *For. Ecosyst.*, 2, 24, <https://doi.org/10.1186/s40663-015-0048-1>, 2015.
- 721 Richter, A., Nakamura, G., Agra-Iserhard, C., and da Silva Duarte, L.: The hidden side of diversity:
722 Effects of imperfect detection on multiple dimensions of biodiversity, *Ecol. Evol.*, 11, 12508–12519,
723 <https://doi.org/10.1002/ece3.7995>, 2021.
- 724 Roth, T., Allan, E., Pearman, P. B., and Amrhein, V.: Functional ecology and imperfect detection of
725 species, *Methods Ecol. Evol.*, 9, 917–928, <https://doi.org/10.1111/2041-210X.12950>, 2018.
- 726 Roth, V. N., Lange, M., Simon, C., Hertkorn, N., Bueher, S., Goodall, T., Griffiths, R. I., Mellado-
727 Vázquez, P. G., Mommer, L., Oram, N. J., Weigelt, A., Dittmar, T., and Gleixner, G.: Persistence of
728 dissolved organic matter explained by molecular changes during its passage through soil, *Nat.*
729 *Geosci.*, 12, 755–761, <https://doi.org/10.1038/s41561-019-0417-4>, 2019.
- 730 Ruddy, B. M., Hendrickson, C. L., Rodgers, R. P., and Marshall, A. G.: Positive Ion Electrospray
731 Ionization Suppression in Petroleum and Complex Mixtures, *Energy Fuels*, 32, 2901–2907,
732 <https://doi.org/10.1021/acs.energyfuels.7b03204>, 2018.
- 733 Senko, M. W., Hendrickson, C. L., Emmett, M. R., Shi, S. D. H., and Marshall, A. G.: External
734 Accumulation of Ions for Enhanced Electrospray Ionization Fourier Transform Ion Cyclotron
735 Resonance Mass Spectrometry, *J. Am. Soc. Mass Spectrom.*, 8, 970–976,
736 [https://doi.org/10.1016/S1044-0305\(97\)00126-8](https://doi.org/10.1016/S1044-0305(97)00126-8), 1997.
- 737 Shaw, J. B., Lin, T. Y., Leach, F. E., Tolmachev, A. V., Tolić, N., Robinson, E. W., Koppelaar, D. W.,
738 and Paša-Tolić, L.: 21 Tesla Fourier Transform Ion Cyclotron Resonance Mass Spectrometer Greatly
739 Expands Mass Spectrometry Toolbox, *J. Am. Soc. Mass Spectrom.*, 27, 1929–1936,
740 <https://doi.org/10.1007/s13361-016-1507-9>, 2016.
- 741 Smith, D. F., Podgorski, D. C., Rodgers, R. P., Blakney, G. T., and Hendrickson, C. L.: 21 Tesla FT-ICR
742 Mass Spectrometer for Ultrahigh Resolution Analysis of Complex Organic Mixtures, *Anal. Chem.*,
743 90, 2041–2047, <https://doi.org/10.1021/acs.analchem.7b04159>, 2018.
- 744 Steen, A. D., Kuseh, S., Abdulla, H. A., Calkić, N., Coffinet, S., Dittmar, T., Fulton, J. M., Galy, V.,
745 Hinrichs, K. U., Ingalls, A. E., Koch, B. P., Kujawinski, E., Liu, Z., Osterholz, H., Rush, D., Seidel,
746 M., Sepúlveda, J., and Wakeham, S. G.: Analytical and Computational Advances, Opportunities, and
747 Challenges in Marine Organic Biogeochemistry in an Era of “Omics,” *Front. Mar. Sci.*, 7, 2020.
- 748 Tanentzap, A. J., Fitch, A., Orland, C., Emilson, E. J. S., Yakimovich, K. M., Osterholz, H., and Dittmar,
749 T.: Chemical and microbial diversity covary in fresh water to influence ecosystem functioning, *Proc.*
750 *Natl. Acad. Sci.*, 116, 24689–24695, <https://doi.org/10.1073/pnas.1904896116>, 2019.
- 751 Tose, L. V., Benigni, P., Leyva, D., Sundberg, A., Ramírez, C. E., Ridgeway, M. E., Park, M. A., Romão,
752 W., Jaffé, R., and Fernandez-Lima, F.: Coupling trapped ion mobility spectrometry to mass
753 spectrometry: trapped ion mobility spectrometry–time of flight mass spectrometry versus trapped ion
754 mobility spectrometry–Fourier transform ion cyclotron resonance mass spectrometry, *Rapid*
755 *Commun. Mass Spectrom.*, 32, 1287–1295, <https://doi.org/10.1002/rem.8165>, 2018.
- 756 Trufelli, H., Palma, P., Famigliini, G., and Cappiello, A.: An overview of matrix effects in liquid
757 chromatography–mass spectrometry, *Mass Spectrom. Rev.*, 30, 491–509,
758 <https://doi.org/10.1002/mas.20298>, 2011.
- 759 Urban, P. L.: Quantitative mass spectrometry: an overview, *Philos. Trans. R. Soc. Math. Phys. Eng. Sci.*,
760 374, 20150382, <https://doi.org/10.1098/rsta.2015.0382>, 2016.
- 761 Vieira-Silva, S., Sabino, J., Valles-Colomer, M., Falony, G., Kathagen, G., Caenepeel, C., Cleynen, J.,

- 762 van der Merwe, S., Vermeire, S., and Raes, J.: Quantitative microbiome profiling disentangles
763 inflammation and bile duct obstruction associated microbiota alterations across PSC/IBD diagnoses,
764 *Nat. Microbiol.*, 4, 1826–1831, <https://doi.org/10.1038/s41564-019-0483-9>, 2019.
- 765 Wen, Z., Shang, Y., Lyu, L., Liu, G., Hou, J., He, C., Shi, Q., He, D., and Song, K.: Sources and
766 composition of riverine dissolved organic matter to marginal seas from mainland China, *J. Hydrol.*,
767 127152, <https://doi.org/10.1016/j.jhydrol.2021.127152>, 2021.
- 768 Whittaker, R. H.: Evolution and Measurement of Species Diversity, *TAXON*, 21, 213–251,
769 <https://doi.org/10.2307/1218190>, 1972.
- 770 Wörner, T. P., Snijder, J., Bennett, A., Agbandje-McKenna, M., Makarov, A. A., and Heck, A. J. R.:
771 Resolving heterogeneous macromolecular assemblies by Orbitrap-based single-particle charge
772 detection mass spectrometry, *Nat. Methods*, 17, 395–398, <https://doi.org/10.1038/s41592-020-0770-7>, 2020.
- 773 Zark, M., Christoffers, J., and Dittmar, T.: Molecular properties of deep-sea dissolved organic matter are
774 predictable by the central limit theorem: Evidence from tandem FT-ICR-MS, *Mar. Chem.*, 191, 9–15,
775 <https://doi.org/10.1016/j.marchem.2017.02.005>, 2017.
- 776 Anderson, M. J., Crist, T. O., Chase, J. M., Vellend, M., Inouye, B. D., Freestone, A. L., Sanders, N. J., Cornell, H. V., Comita, L. S., Davies, K. F., Harrison, S. P.,
777 Kraft, N. J. B., Stegen, J. C., and Swenson, N. G.: Navigating the multiple meanings of β diversity: a roadmap
778 for the practicing ecologist, *Ecol. Lett.*, 14, 19–28, <https://doi.org/10.1111/j.1461-0248.2010.01552.x>, 2011.
- 779 Bahureksa, W., Tfaily, M. M., Boiteau, R. M., Young, R. B., Logan, M. N., McKenna, A. M., and Borch, T.: Soil
780 Organic Matter Characterization by Fourier Transform Ion Cyclotron Resonance Mass Spectrometry (FTICR
781 MS): A Critical Review of Sample Preparation, Analysis, and Data Interpretation, *Environ. Sci. Technol.*, 55,
782 9637–9656, <https://doi.org/10.1021/acs.est.1c01135>, 2021.
- 783 Bao, H., Niggemann, J., Luo, L., Dittmar, T., and Kao, S.-J.: Molecular composition and origin of water-soluble
784 organic matter in marine aerosols in the Pacific off China, *Atmos. Environ.*, 191, 27–35,
785 <https://doi.org/10.1016/j.atmosenv.2018.07.059>, 2018.
- 786 Bhatia, M. P., Das, S. B., Longnecker, K., Charette, M. A., and Kujawinski, E. B.: Molecular characterization of
787 dissolved organic matter associated with the Greenland ice sheet, *Geochim. Cosmochim. Acta.*, 74, 3768–3784,
788 <https://doi.org/10.1016/j.gca.2010.03.035>, 2010.
- 789 Boye, K., Noël, V., Tfaily, M. M., Bone, S. E., Williams, K. H., Bargar, J. R., and Fendorf, S.: Thermodynamically
790 controlled preservation of organic carbon in floodplains, *Nat. Geosci.*, 10, 415–419,
791 <https://doi.org/10.1038/ngeo2940>, 2017.
- 792 Cao, D., Lv, J., Geng, F., Rao, Z., Niu, H., Shi, Y., Cai, Y., and Kang, Y.: Ion Accumulation Time Dependent
793 Molecular Characterization of Natural Organic Matter Using Electrospray Ionization-Fourier Transform Ion
794 Cyclotron Resonance Mass Spectrometry, *Anal. Chem.*, 88, 12210–12218,
795 <https://doi.org/10.1021/acs.analchem.6b03198>, 2016.
- 796 Cooper, W. T., Chanton, J. C., D'Andrilli, J., Hodgkins, S. B., Podgorski, D. C., Stenson, A. C., Tfaily, M. M., and
797 Wilson, R. M.: A History of Molecular Level Analysis of Natural Organic Matter by FTICR Mass Spectrometry
798 and The Paradigm Shift in Organic Geochemistry, *Mass Spectrom. Rev.*, 41, 215–239,
799 <https://doi.org/10.1002/mas.21663>, 2022.
- 800 Danczak, R. E., Chu, R. K., Fansler, S. J., Goldman, A. E., Graham, E. B., Tfaily, M. M., Toyoda, J., and Stegen, J.
801 C.: Using metacommunity ecology to understand environmental metabolomes, *Nat. Commun.*, 11, 6369,
802 <https://doi.org/10.1038/s41467-020-19989-y>, 2020.
- 803 Danczak, R. E., Goldman, A. E., Chu, R. K., Toyoda, J. G., Garayburu-Caruso, V. A., Tolić, N., Graham, E. B.,
804 Morad, J. W., Renteria, L., Wells, J. R., Herzog, S. P., Ward, A. S., and Stegen, J. C.: Ecological theory applied
805 to environmental metabolomes reveals compositional divergence despite conserved molecular properties, *Sci.*
806 *Total Environ.*, 788, 147409, <https://doi.org/10.1016/j.scitotenv.2021.147409>, 2021.
- 807 Derrien, M., Lee, Y. K., Shin, K.-H., and Hur, J.: Comparing discrimination capabilities of fluorescence
808 spectroscopy versus FT-ICR-MS for sources and hydrophobicity of sediment organic matter, *Environ. Sci.*
809 *Pollut. Res.*, 25, 1892–1902, <https://doi.org/10.1007/s11356-017-0531-z>, 2018.
- 810 Dorazio, R. M. and Royle, J. A.: Estimating Size and Composition of Biological Communities by Modeling the
811 Occurrence of Species, *J. Am. Stat. Assoc.*, 100, 389–398, <https://doi.org/10.1198/016214505000000015>, 2005.
- 812 Elliott, K. J., Boring, L. R., Swank, W. T., and Haines, B. R.: Successional changes in plant species diversity and
813 composition after clearcutting a Southern Appalachian watershed, *For. Ecol. Manag.*, 92, 67–85,
814 [https://doi.org/10.1016/S0378-1127\(96\)03947-3](https://doi.org/10.1016/S0378-1127(96)03947-3), 1997.
- 815

- 816 Garayburu-Caruso, V. A., Stegen, J. C., Song, H.-S., Renteria, L., Wells, J., Garcia, W., Resch, C. T., Goldman, A.
817 E., Chu, R. K., Toyoda, J., and Graham, E. B.: Carbon Limitation Leads to Thermodynamic Regulation of
818 Aerobic Metabolism, *Environ. Sci. Technol. Lett.*, 7, 517–524, <https://doi.org/10.1021/acs.estlett.0c00258>,
819 2020.
- 820 Gloor, G. B., Macklaim, J. M., Pawlowsky-Glahn, V., and Egozcue, J. J.: Microbiome Datasets Are Compositional:
821 And This Is Not Optional, *Front. Microbiol.*, 8, 2017.
- 822 Han, L., Kaesler, J., Peng, C., Reemtsma, T., and Lechtenfeld, O. J.: Online Counter Gradient LC-FT-ICR-MS
823 Enables Detection of Highly Polar Natural Organic Matter Fractions, *Anal. Chem.*, 93, 1740–1748,
824 <https://doi.org/10.1021/acs.analchem.0c04426>, 2021.
- 825 Hardwick, S. A., Chen, W. Y., Wong, T., Kanakamedala, B. S., Deveson, I. W., Ongley, S. E., Santini, N. S.,
826 Marcellin, E., Smith, M. A., Nielsen, L. K., Lovelock, C. E., Neilan, B. A., and Mercer, T. R.: Synthetic
827 microbe communities provide internal reference standards for metagenome sequencing and analysis, *Nat.*
828 *Commun.*, 9, 3096, <https://doi.org/10.1038/s41467-018-05555-0>, 2018.
- 829 Hawkes, J. A. and Kew, W.: 4 - High-resolution mass spectrometry strategies for the investigation of dissolved
830 organic matter, in: *Multidimensional Analytical Techniques in Environmental Research*, edited by: Duarte, R.,
831 M. B. O. and Duarte, A. C., Elsevier, 71–104, <https://doi.org/10.1016/B978-0-12-818896-5.00004-1>, 2020a.
- 832 Hawkes, J. A. and Kew, W.: 4 - High-resolution mass spectrometry strategies for the investigation of dissolved
833 organic matter, in: *Multidimensional Analytical Techniques in Environmental Research*, edited by: Duarte, R.,
834 M. B. O. and Duarte, A. C., Elsevier, 71–104, <https://doi.org/10.1016/B978-0-12-818896-5.00004-1>, 2020b.
- 835 Hawkes, J. A., Dittmar, T., Patriarca, C., Tranvik, L., and Bergquist, J.: Evaluation of the Orbitrap Mass
836 Spectrometer for the Molecular Fingerprinting Analysis of Natural Dissolved Organic Matter, *Anal. Chem.*, 88,
837 7698–7704, <https://doi.org/10.1021/acs.analchem.6b01624>, 2016.
- 838 Hedges, J. I., Eglinton, G., Hatcher, P. G., Kirchman, D. L., Arnosti, C., Derenne, S., Evershed, R. P., Kögel-
839 Knabner, I., de Leeuw, J. W., Littke, R., Michaelis, W., and Rullkötter, J.: The molecularly-uncharacterized
840 component of nonliving organic matter in natural environments, *Org. Geochem.*, 31, 945–958,
841 [https://doi.org/10.1016/S0146-6380\(00\)00096-6](https://doi.org/10.1016/S0146-6380(00)00096-6), 2000.
- 842 Hill, M. O.: Diversity and Evenness: A Unifying Notation and Its Consequences, *Ecology*, 54, 427–432,
843 <https://doi.org/10.2307/1934352>, 1973.
- 844 Iknayan, K. J., Tingley, M. W., Furnas, B. J., and Beissinger, S. R.: Detecting diversity: emerging methods to
845 estimate species diversity, *Trends Ecol. Evol.*, 29, 97–106, <https://doi.org/10.1016/j.tree.2013.10.012>, 2014.
- 846 Kaiser, N. K., McKenna, A. M., Savory, J. J., Hendrickson, C. L., and Marshall, A. G.: Tailored Ion Radius
847 Distribution for Increased Dynamic Range in FT-ICR Mass Analysis of Complex Mixtures, *Anal. Chem.*, 85,
848 265–272, <https://doi.org/10.1021/ac302678v>, 2013.
- 849 Kellerman, A. M., Dittmar, T., Kothawala, D. N., and Tranvik, L. J.: Chemodiversity of dissolved organic matter in
850 lakes driven by climate and hydrology, *Nat. Commun.*, 5, 3804, <https://doi.org/10.1038/ncomms4804>, 2014.
- 851 Kim, D., Kim, S., Son, S., Jung, M.-J., and Kim, S.: Application of Online Liquid Chromatography 7 T FT-ICR
852 Mass Spectrometer Equipped with Quadrupolar Detection for Analysis of Natural Organic Matter, *Anal. Chem.*,
853 91, 7690–7697, <https://doi.org/10.1021/acs.analchem.9b00689>, 2019.
- 854 Krueve, A.: Strategies for Drawing Quantitative Conclusions from Nontargeted Liquid Chromatography–High-
855 Resolution Mass Spectrometry Analysis, *Anal. Chem.*, 92, 4691–4699,
856 <https://doi.org/10.1021/acs.analchem.9b03481>, 2020.
- 857 Krueve, A., Kaupmees, K., Liigand, J., and Leito, I.: Negative Electrospray Ionization via Deprotonation: Predicting
858 the Ionization Efficiency, *Anal. Chem.*, 86, 4822–4830, <https://doi.org/10.1021/ac404066v>, 2014.
- 859 Kujawinski, E. B.: Electrospray Ionization Fourier Transform Ion Cyclotron Resonance Mass Spectrometry (ESI
860 FT-ICR MS): Characterization of Complex Environmental Mixtures, *Environ. Forensics*, 3, 207–216,
861 <https://doi.org/10.1006/enfo.2002.0109>, 2002.
- 862 Kujawinski, E. B., Longnecker, K., Blough, N. V., Vecchio, R. D., Finlay, L., Kitner, J. B., and Giovannoni, S. J.:
863 Identification of possible source markers in marine dissolved organic matter using ultrahigh resolution mass
864 spectrometry, *Geochim. Cosmochim. Acta*, 73, 4384–4399, <https://doi.org/10.1016/j.gca.2009.04.033>, 2009.
- 865 Laliberté, E. and Legendre, P.: A distance-based framework for measuring functional diversity from multiple traits,
866 *Ecology*, 91, 299–305, <https://doi.org/10.1890/08-2244.1>, 2010.
- 867 LaRowe, D. E. and Van Cappellen, P.: Degradation of natural organic matter: A thermodynamic analysis, *Geochim.*
868 *Cosmochim. Acta*, 75, 2030–2042, <https://doi.org/10.1016/j.gca.2011.01.020>, 2011.
- 869 Lavorel, S., Grigulis, K., McIntyre, S., Williams, N. S. G., Garden, D., Dorrough, J., Berman, S., Ouetier, F.,
870 Thébault, A., and Bonis, A.: Assessing functional diversity in the field – methodology matters!, *Funct. Ecol.*,
871 22, 134–147, <https://doi.org/10.1111/j.1365-2435.2007.01339.x>, 2008.

- 872 [Leyva, D., Tose, L. V., Porter, J., Wolff, J., Jaffé, R., and Fernandez-Lima, F.: Understanding the structural](#)
873 [complexity of dissolved organic matter: isomeric diversity, *Faraday Discuss.*, 218, 431–440,](#)
874 <https://doi.org/10.1039/C8FD00221E>, 2019.
- 875 [Leyva, D., Jaffe, R., and Fernandez-Lima, F.: Structural Characterization of Dissolved Organic Matter at the](#)
876 [Chemical Formula Level Using TIMS-FT-ICR MS/MS, *Anal. Chem.*, 92, 11960–11966,](#)
877 <https://doi.org/10.1021/acs.analchem.0c02347>, 2020.
- 878 [Li, H.-Y., Wang, H., Wang, H.-T., Xin, P.-Y., Xu, X.-H., Ma, Y., Liu, W.-P., Teng, C.-Y., Jiang, C.-L., Lou, L.-P.,](#)
879 [Arnold, W., Cralle, L., Zhu, Y.-G., Chu, J.-F., Gilbert, J. A., and Zhang, Z.-J.: The chemodiversity of paddy soil](#)
880 [dissolved organic matter correlates with microbial community at continental scales, *Microbiome*, 6, 187,](#)
881 <https://doi.org/10.1186/s40168-018-0561-x>, 2018.
- 882 [Li, Y., Harir, M., Uhl, J., Kanawati, B., Lucio, M., Smirnov, K. S., Koch, B. P., Schmitt-Kopplin, P., and Hertkorn,](#)
883 [N.: How representative are dissolved organic matter \(DOM\) extracts? A comprehensive study of sorbent](#)
884 [selectivity for DOM isolation, *Water Res.*, 116, 316–323, <https://doi.org/10.1016/j.watres.2017.03.038>, 2017.](#)
- 885 [Lucas, J., Koester, I., Wichels, A., Niggemann, J., Dittmar, T., Callies, U., Wiltshire, K. H., and Gerdts, G.: Short-](#)
886 [Term Dynamics of North Sea Bacterioplankton-Dissolved Organic Matter Coherence on Molecular Level,](#)
887 [*Front. Microbiol.*, 7, 2016.](#)
- 888 [Makarov, A., Denisov, E., Kholomeev, A., Balschun, W., Lange, O., Strupat, K., and Horning, S.: Performance](#)
889 [Evaluation of a Hybrid Linear Ion Trap/Orbitrap Mass Spectrometer, *Anal. Chem.*, 78, 2113–2120,](#)
890 <https://doi.org/10.1021/ac0518811>, 2006.
- 891 [Makarov, A., Grinfeld, D., and Ayzikov, K.: Chapter 2 - Fundamentals of Orbitrap analyzer, in: *Fundamentals and*](#)
892 [Applications of Fourier Transform Mass Spectrometry](#), edited by: Kanawati, B. and Schmitt-Kopplin, P.,
893 [Elsevier, 37–61, <https://doi.org/10.1016/B978-0-12-814013-0.00002-8>, 2019.](#)
- 894 [Marshall, A. G., Hendrickson, C. L., and Jackson, G. S.: Fourier transform ion cyclotron resonance mass](#)
895 [spectrometry: A primer, *Mass Spectrom. Rev.*, 17, 1–35, \[https://doi.org/10.1002/\\(SICI\\)1098-\]\(https://doi.org/10.1002/\(SICI\)1098-\)](#)
896 [2787\(1998\)17:1<1::AID-MAS1>3.0.CO;2-K](#), 1998.
- 897 [McGill, B. J., Enquist, B. J., Weiher, E., and Westoby, M.: Rebuilding community ecology from functional traits,](#)
898 [*Trends Ecol. Evol.*, 21, 178–185, <https://doi.org/10.1016/j.tree.2006.02.002>, 2006.](#)
- 899 [McGill, B. J., Etienne, R. S., Gray, J. S., Alonso, D., Anderson, M. J., Benecha, H. K., Dornelas, M., Enquist, B. J.,](#)
900 [Green, J. L., He, F., Hurlbert, A. H., Magurran, A. E., Marquet, P. A., Maurer, B. A., Ostling, A., Soykan, C.,](#)
901 [U., Ugland, K. I., and White, E. P.: Species abundance distributions: moving beyond single prediction theories](#)
902 [to integration within an ecological framework, *Ecol. Lett.*, 10, 995–1015, <https://doi.org/10.1111/j.1461->](#)
903 [0248.2007.01094.x](#), 2007.
- 904 [Merder, J., Röder, H., Dittmar, T., Feudel, U., Freund, J. A., Gerdts, G., Kraberg, A., and Niggemann, J.: Dissolved](#)
905 [organic compounds with synchronous dynamics share chemical properties and origin, *Limnol. Oceanogr.*, n/a,](#)
906 <https://doi.org/10.1002/lno.11938>, 2021.
- 907 [Mouillot, D. and Leprêtre, A.: A comparison of species diversity estimators, *Res. Popul. Ecol.*, 41, 203–215,](#)
908 <https://doi.org/10.1007/s101440050024>, 1999.
- 909 [Muscarella, R. and Uriarte, M.: Do community-weighted mean functional traits reflect optimal strategies?, *Proc. R.*](#)
910 [Soc. B Biol. Sci.](#), 283, 20152434, <https://doi.org/10.1098/rspb.2015.2434>, 2016.
- 911 [Osterholz, H., Singer, G., Wemheuer, B., Daniel, R., Simon, M., Niggemann, J., and Dittmar, T.: Deciphering](#)
912 [associations between dissolved organic molecules and bacterial communities in a pelagic marine system, *ISME*](#)
913 [J.](#), 10, 1717–1730, <https://doi.org/10.1038/ismej.2015.231>, 2016.
- 914 [Raeke, J., Lechtenfeld, O. J., Wagner, M., Herzsprung, P., and Reemtsma, T.: Selectivity of solid phase extraction of](#)
915 [freshwater dissolved organic matter and its effect on ultrahigh resolution mass spectra, *Environ. Sci. Process.*](#)
916 [Impacts](#), 18, 918–927, <https://doi.org/10.1039/C6EM00200E>, 2016.
- 917 [Redowan, M.: Spatial pattern of tree diversity and evenness across forest types in Majella National Park, Italy, *For.*](#)
918 [Ecosyst.](#), 2, 24, <https://doi.org/10.1186/s40663-015-0048-1>, 2015.
- 919 [Richter, A., Nakamura, G., Agra Iserhard, C., and da Silva Duarte, L.: The hidden side of diversity: Effects of](#)
920 [imperfect detection on multiple dimensions of biodiversity, *Ecol. Evol.*, 11, 12508–12519,](#)
921 <https://doi.org/10.1002/ece3.7995>, 2021.
- 922 [Roth, T., Allan, E., Pearman, P. B., and Amrhein, V.: Functional ecology and imperfect detection of species,](#)
923 [*Methods Ecol. Evol.*, 9, 917–928, <https://doi.org/10.1111/2041-210X.12950>, 2018.](#)
- 924 [Roth, V.-N., Lange, M., Simon, C., Hertkorn, N., Bucher, S., Goodall, T., Griffiths, R. I., Mellado-Vázquez, P. G.,](#)
925 [Mommer, L., Oram, N. J., Weigelt, A., Dittmar, T., and Gleixner, G.: Persistence of dissolved organic matter](#)
926 [explained by molecular changes during its passage through soil, *Nat. Geosci.*, 12, 755–761,](#)
927 <https://doi.org/10.1038/s41561-019-0417-4>, 2019.

- 928 Ruddy, B. M., Hendrickson, C. L., Rodgers, R. P., and Marshall, A. G.: Positive Ion Electrospray Ionization
 929 Suppression in Petroleum and Complex Mixtures, *Energy Fuels*, 32, 2901–2907,
 930 <https://doi.org/10.1021/acs.energyfuels.7b03204>, 2018.
- 931 Sakas, J., Kitson, E., Bell, N. G. A., and Uhrin, D.: MS and NMR Analysis of Isotopically Labeled Chloramination
 932 Disinfection Byproducts: Hyperlinks and Chemical Reactions, *Anal. Chem.*, 96, 8263–8272,
 933 <https://doi.org/10.1021/acs.analchem.3c03888>, 2024.
- 934 Senko, M. W., Hendrickson, C. L., Emmett, M. R., Shi, S. D.-H., and Marshall, A. G.: External Accumulation of
 935 Ions for Enhanced Electrospray Ionization Fourier Transform Ion Cyclotron Resonance Mass Spectrometry, *J.*
 936 *Am. Soc. Mass Spectrom.*, 8, 970–976, [https://doi.org/10.1016/S1044-0305\(97\)00126-8](https://doi.org/10.1016/S1044-0305(97)00126-8), 1997.
- 937 Shaw, J. B., Lin, T.-Y., Leach, F. E., Tolmachev, A. V., Tolić, N., Robinson, E. W., Koppelaar, D. W., and Paša-
 938 Tolić, L.: 21 Tesla Fourier Transform Ion Cyclotron Resonance Mass Spectrometer Greatly Expands Mass
 939 Spectrometry Toolbox, *J. Am. Soc. Mass Spectrom.*, 27, 1929–1936, [https://doi.org/10.1007/s13361-016-1507-](https://doi.org/10.1007/s13361-016-1507-9)
 940 9, 2016.
- 941 Smith, D. F., Podgorski, D. C., Rodgers, R. P., Blakney, G. T., and Hendrickson, C. L.: 21 Tesla FT-ICR Mass
 942 Spectrometer for Ultrahigh-Resolution Analysis of Complex Organic Mixtures, *Anal. Chem.*, 90, 2041–2047,
 943 <https://doi.org/10.1021/acs.analchem.7b04159>, 2018.
- 944 Spencer, R. G. M., Mann, P. J., Dittmar, T., Eglinton, T. I., McIntyre, C., Holmes, R. M., Zimov, N., and Stubbins,
 945 A.: Detecting the signature of permafrost thaw in Arctic rivers, *Geophys. Res. Lett.*, 42, 2830–2835,
 946 <https://doi.org/10.1002/2015GL063498>, 2015.
- 947 Steen, A. D., Kusch, S., Abdulla, H. A., Cakić, N., Coffinet, S., Dittmar, T., Fulton, J. M., Galy, V., Hinrichs, K.-U.,
 948 Ingalls, A. E., Koch, B. P., Kujawinski, E., Liu, Z., Osterholz, H., Rush, D., Seidel, M., Sepúlveda, J., and
 949 Wakeham, S. G.: Analytical and Computational Advances, Opportunities, and Challenges in Marine Organic
 950 Biogeochemistry in an Era of “Omics,” *Front. Mar. Sci.*, 7, 2020.
- 951 Stubbins, A., Spencer, R. G. M., Chen, H., Hatcher, P. G., Mopper, K., Hernes, P. J., Mwamba, V. L., Mangangu, A.
 952 M., Wabakghanzi, J. N., and Six, J.: Illuminated darkness: Molecular signatures of Congo River dissolved
 953 organic matter and its photochemical alteration as revealed by ultrahigh precision mass spectrometry, *Limnol.*
 954 *Oceanogr.*, 55, 1467–1477, <https://doi.org/10.4319/lo.2010.55.4.1467>, 2010.
- 955 Tanentzap, A. J., Fitch, A., Orland, C., Emilson, E. J. S., Yakimovich, K. M., Osterholz, H., and Dittmar, T.:
 956 Chemical and microbial diversity covary in fresh water to influence ecosystem functioning, *Proc. Natl. Acad.*
 957 *Sci.*, 116, 24689–24695, <https://doi.org/10.1073/pnas.1904896116>, 2019.
- 958 Thompson, A. M., Stratton, K. G., Bramer, L. M., Zavoshy, N. S., and McCue, L. A.: Fourier transform ion
 959 cyclotron resonance mass spectrometry (FT-ICR-MS) peak intensity normalization for complex mixture
 960 analyses, *Rapid Commun. Mass Spectrom.*, 35, e9068, <https://doi.org/10.1002/rcm.9068>, 2021.
- 961 Tose, L. V., Benigni, P., Leyva, D., Sundberg, A., Ramírez, C. E., Ridgeway, M. E., Park, M. A., Romão, W., Jaffé,
 962 R., and Fernandez-Lima, F.: Coupling trapped ion mobility spectrometry to mass spectrometry: trapped ion
 963 mobility spectrometry–time-of-flight mass spectrometry versus trapped ion mobility spectrometry–Fourier
 964 transform ion cyclotron resonance mass spectrometry, *Rapid Commun. Mass Spectrom.*, 32, 1287–1295,
 965 <https://doi.org/10.1002/rcm.8165>, 2018.
- 966 Trufelli, H., Palma, P., Famigliani, G., and Cappiello, A.: An overview of matrix effects in liquid chromatography–
 967 mass spectrometry, *Mass Spectrom. Rev.*, 30, 491–509, <https://doi.org/10.1002/mas.20298>, 2011.
- 968 Urban, P. L.: Quantitative mass spectrometry: an overview, *Philos. Trans. R. Soc. Math. Phys. Eng. Sci.*, 374,
 969 20150382, <https://doi.org/10.1098/rsta.2015.0382>, 2016.
- 970 Vieira-Silva, S., Sabino, J., Valles-Colomer, M., Falony, G., Kathagen, G., Caenepael, C., Cleynen, I., van der
 971 Merwe, S., Vermeire, S., and Raes, J.: Quantitative microbiome profiling disentangles inflammation- and bile
 972 duct obstruction-associated microbiota alterations across PSC/IBD diagnoses, *Nat. Microbiol.*, 4, 1826–1831,
 973 <https://doi.org/10.1038/s41564-019-0483-9>, 2019.
- 974 Villéger, S., Brosse, S., Mouchet, M., Mouillot, D., and Vanni, M. J.: Functional ecology of fish: current approaches
 975 and future challenges, *Aquat. Sci.*, 79, 783–801, <https://doi.org/10.1007/s00027-017-0546-z>, 2017.
- 976 Violle, C., Navas, M.-L., Vile, D., Kazakou, E., Fortunel, C., Hummel, I., and Garnier, E.: Let the concept of trait be
 977 functional!, *Oikos*, 116, 882–892, <https://doi.org/10.1111/j.0030-1299.2007.15559.x>, 2007.
- 978 Wen, Z., Shang, Y., Lyu, L., Liu, G., Hou, J., He, C., Shi, Q., He, D., and Song, K.: Sources and composition of
 979 riverine dissolved organic matter to marginal seas from mainland China, *J. Hydrol.*, 127152,
 980 <https://doi.org/10.1016/j.jhydrol.2021.127152>, 2021.
- 981 Whittaker, R. H.: Evolution and Measurement of Species Diversity, *TAXON*, 21, 213–251,
 982 <https://doi.org/10.2307/1218190>, 1972.
- 983 Wörner, T. P., Snijder, J., Bennett, A., Agbandje-McKenna, M., Makarov, A. A., and Heck, A. J. R.: Resolving

984 [heterogeneous macromolecular assemblies by Orbitrap-based single-particle charge detection mass](#)
985 [spectrometry, Nat. Methods, 17, 395–398, <https://doi.org/10.1038/s41592-020-0770-7>, 2020.](#)
986 [Zark, M., Christoffers, J., and Dittmar, T.: Molecular properties of deep-sea dissolved organic matter are predictable](#)
987 [by the central limit theorem: Evidence from tandem FT-ICR-MS, Mar. Chem., 191, 9–15,](#)
988 [https://doi.org/10.1016/j.marchem.2017.02.005, 2017.](#)

989
990

Figures

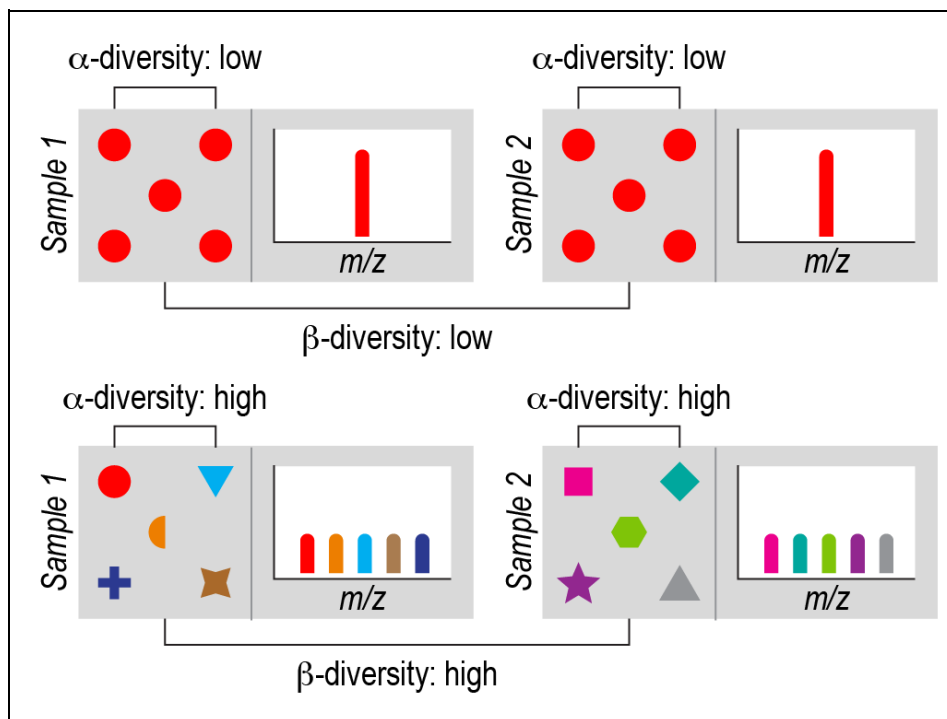


Figure 1. Ecological concepts of α -diversity and β -diversity. Each gray box represents a sample of an ecological community or collection of organic molecules (i.e., [an OM₄NOM assemblage](#)). Symbols represent individual organisms or molecules. Different biological or molecular species are represented by a combination of shape and color. (Top) Each sample has one biological species (red circles) or one chemical species (red bar), and the species are the same within and between the samples. This reflects minimal α -diversity because there is a single species. This also reflects minimal β -diversity because there is no difference in which species are present in each sample. (Bottom) Each sample has five species (biological or chemical) represented by different colors and symbols. There are no shared species between samples. This reflects maximum α -diversity because every individual is a different species within each sample, and maximum β -diversity because there are no species shared between samples. In real ecological and [OM₄NOM](#) samples, α -diversity and β -diversity fall between these extremes.

991
992

Formatted: Header

Formatted Table

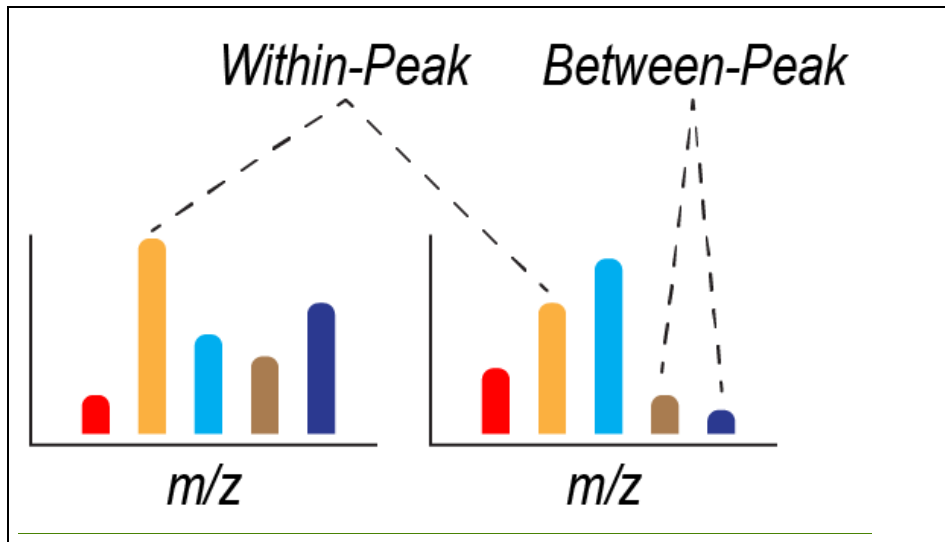


Figure 2. Summary of within-peak and between-peak comparisons of peak intensity. Two idealized mass spectra (i.e., from two samples) are shown with each peak defined by a mass-to-charge ratio (m/z) and represented by a different color. The intensity of each peak in each sample is represented by the height of each colored bar. Within-peak comparisons of intensity are based on comparing intensities at the same m/z across two or more samples. Between-peak comparisons of intensity are based on comparing intensities at two or more m/z values. Between-peak comparisons can be done within a sample (as shown) or between samples (not shown).

993

Formatted: Header

Formatted Table

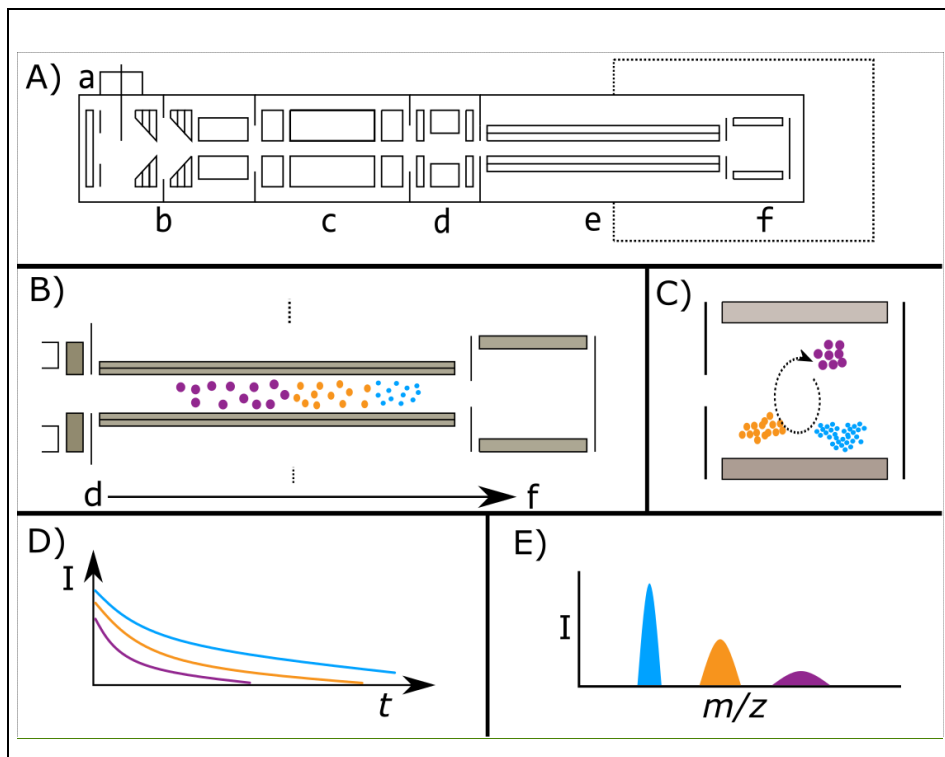
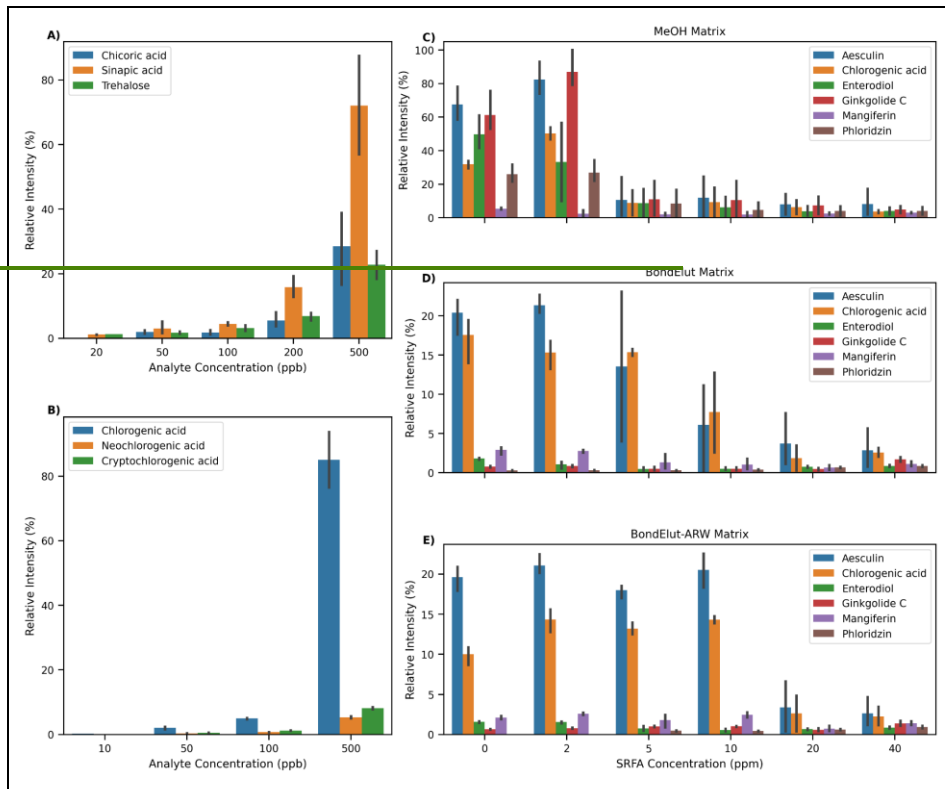


Figure 3. Illustrative example of a generic FTICR mass spectrometer (panel A), showing common and key biases between FTICR signal intensity and m/z of ions (B-E). Panel A shows the major elements of a generic FTICR mass spectrometer (based loosely on a Bruker solarix FTICR MS geometry). Panel A elements include; a - atmospheric pressure ionization source (i.e. ESI source), b - source ion optics (i.e. dual ion funnels), c - mass selecting quadrupole, d - collision cell, e - transfer multipoles to ICR cell, f - ICR cell. Dashed line indicates the magnetic field. Note: diagram is deliberately simplified and not to scale. Panel B) demonstrates the time-of-flight bias along the transfer multipoles (e) in the 'flight tube', from the collision cell (d) to the ICR cell (f). Lower m/z ions travel faster, as indicated by the smaller icons reaching the ICR cell first. Ions are shaded to aid visualization. Panel C) visualizes the effect of a variable excitation radii for ions of different masses, as may happen with a CHIRP excitation pulse. Lower m/z ions are closer to the detection electrodes (shaded in gray) and therefore will induce a larger image current. Note also the ion populations have been adjusted from B) to indicate biases from the time-of-flight effect. Panel D) shows the time-domain recorded signal intensity against time, with the ions having an initial intensity roughly proportional to the number of ions in that cloud. However, as time progresses the less abundant ion clouds lose coherence and destabilize more rapidly, resulting in an attenuation of their signal. Note that the real signal would follow a damped sinusoidal function; here an absolute value approximation is shown for simplicity. Panel E) shows the mass spectrum post-Fourier transform, demonstrating that the impact is not only on peak intensity (peak shown as height), but also peak resolution (peak shown as width). In all cases, effects are deliberately exaggerated and not-to-scale to aid interpretation.

Formatted: Header



Formatted Table

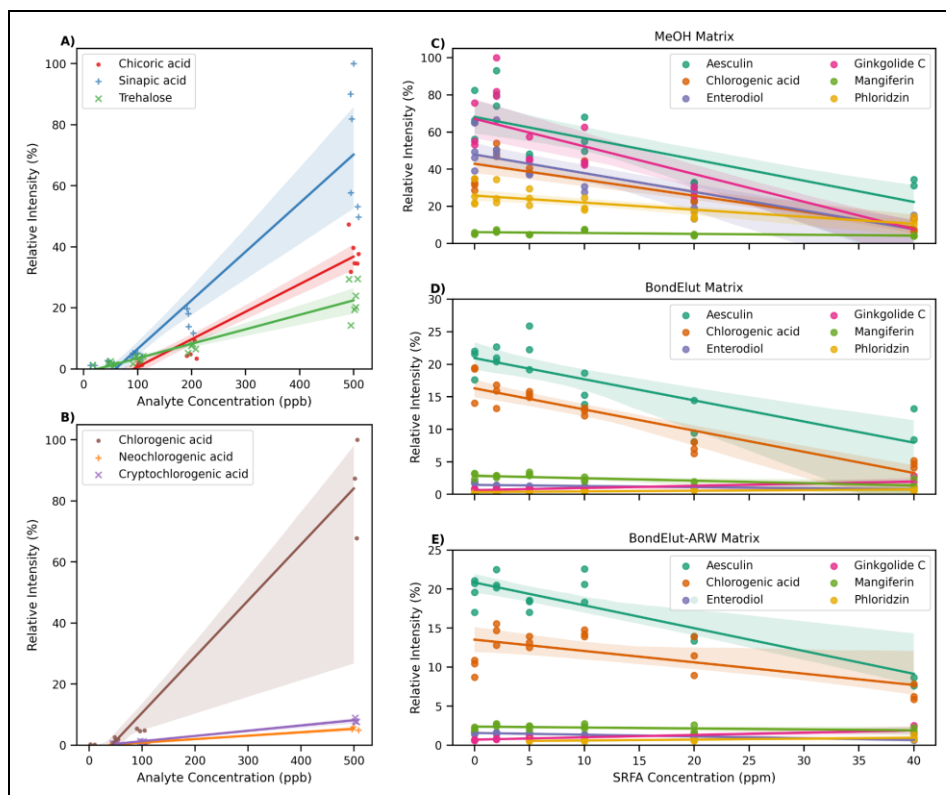


Figure 4 - A) Scatterplot visualization of the relationship between signal intensity (relative intensity) and concentration of analyte for three chemically distinct molecules analyzed contemporaneously but independently in pure methanol solvent. Relative intensity indicates data were scaled to the largest signal in any replicate from the associated series of spectra. Replicates are combined to show their mean. Linear regression and 95% confidence intervals calculated by the Seaborn plotting library with default settings. X-axis jitter was added to aid visualization of overlapping points. B) As with A), but for three structural isomers of chlorogenic acid. X-axis jitter was added to aid visualization of overlapping points. C-E) Compounds spiked into three different solvent matrices (methanol, BondElut methanol, and BondElut artificial river water (ARW)) at a fixed concentration (100 ppb), but with addition of SRFA at varying concentrations from 0 to 40 ppm. In all cases, [M-H]⁻ ion only is shown, but other ions (i.e. [M+Cl]⁻) were detected. 95% confidence intervals represent the results of triplicate measurements. Intensities/Relative intensities have been scaled per plot for A and B, and are on the same scale for C-E). Pearson R correlation coefficients and p-values are reported in Table S1.

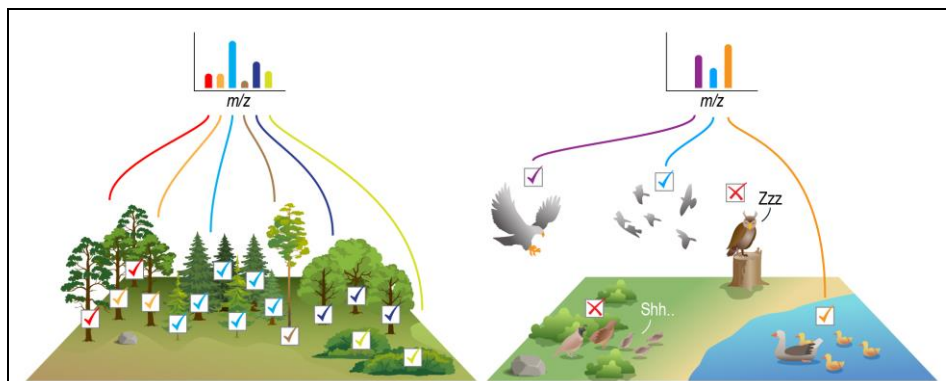


Figure 5. Graphical summary of how FTMS peak intensity data are often treated (left), which is distinct from the reality of those data (right). When surveying the number of individuals of each species within a tree community, there is good confidence that the measured abundances are close to real abundances. This is because there is relatively little variation across species in the ability to detect individuals. FTMS peak intensity data are often used as though they are like tree-community data. However, FTMS data are more like bird-community data. That is, the ability to detect different species varies due to intrinsic factors (e.g., activity patterns, how loud and often birds call, etc.) and extrinsic factors (e.g., habitat structural complexity, predator-induced behavioral changes, etc.). Similarly, the intrinsic physics of a given molecule will impact its ability to ionize and thus its observed peak intensity, and in environmental samples there are thousands of molecular species that impact the ionization 'behavior' of each other. FTMS data being more bird-like than tree-like needs to be accounted for when performing ecological analyses using FTMS data.

997

Formatted: Header

Formatted Table

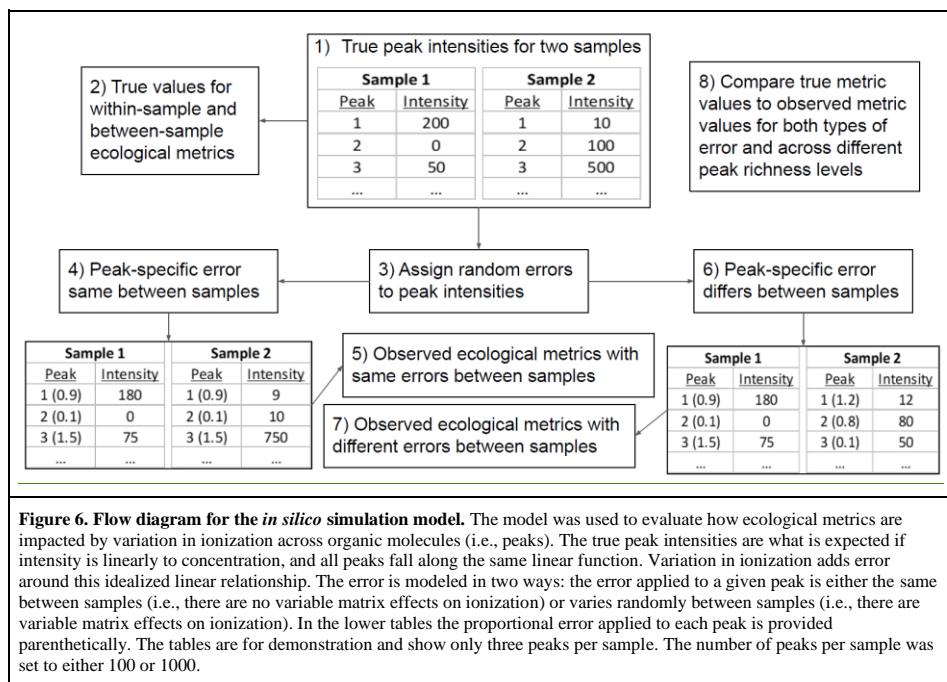


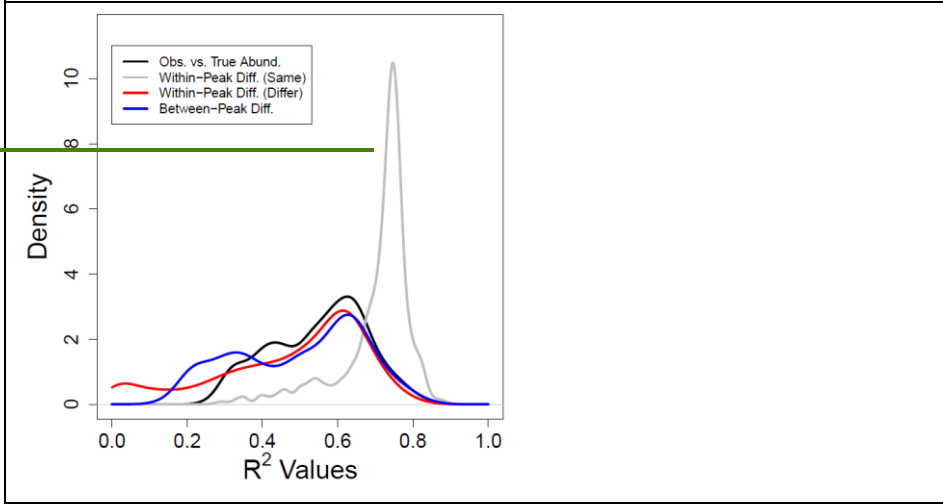
Figure 6. Flow diagram for the *in silico* simulation model. The model was used to evaluate how ecological metrics are impacted by variation in ionization across organic molecules (i.e., peaks). The true peak intensities are what is expected if intensity is linearly to concentration, and all peaks fall along the same linear function. Variation in ionization adds error around this idealized linear relationship. The error is modeled in two ways: the error applied to a given peak is either the same between samples (i.e., there are no variable matrix effects on ionization) or varies randomly between samples (i.e., there are variable matrix effects on ionization). In the lower tables the proportional error applied to each peak is provided parenthetically. The tables are for demonstration and show only three peaks per sample. The number of peaks per sample was set to either 100 or 1000.

Formatted: Header

Formatted Table

|

1000



Formatted: Header

Formatted: Left

Formatted Table

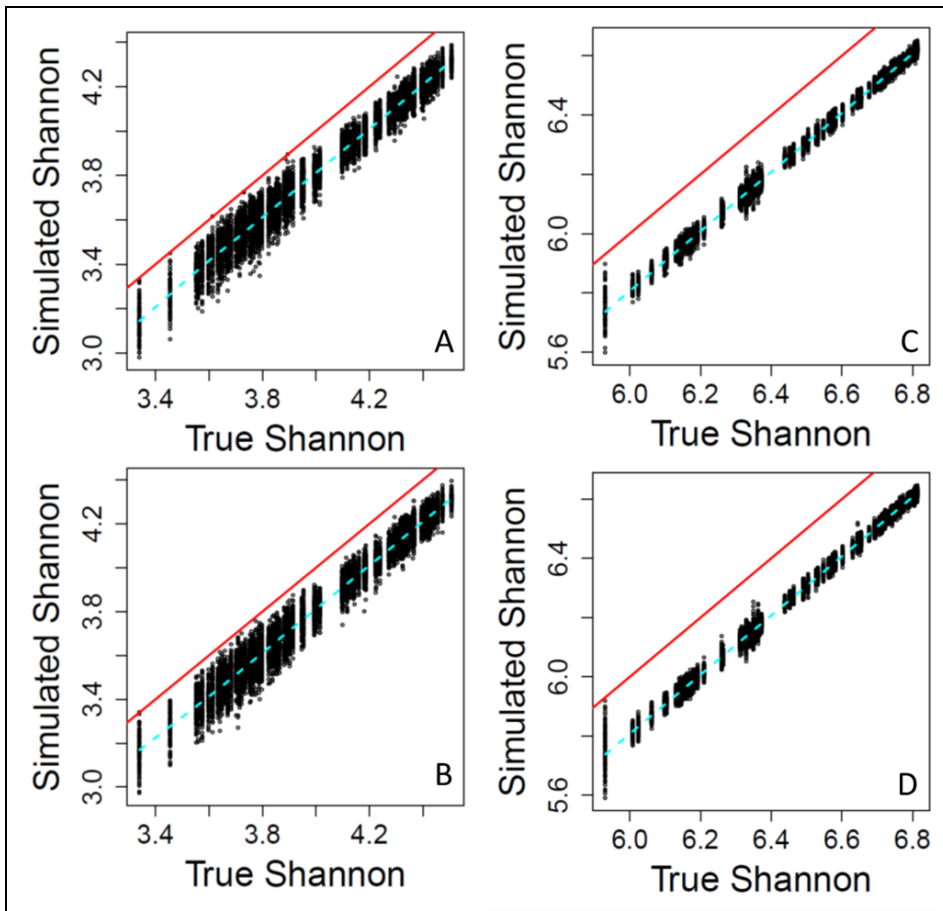
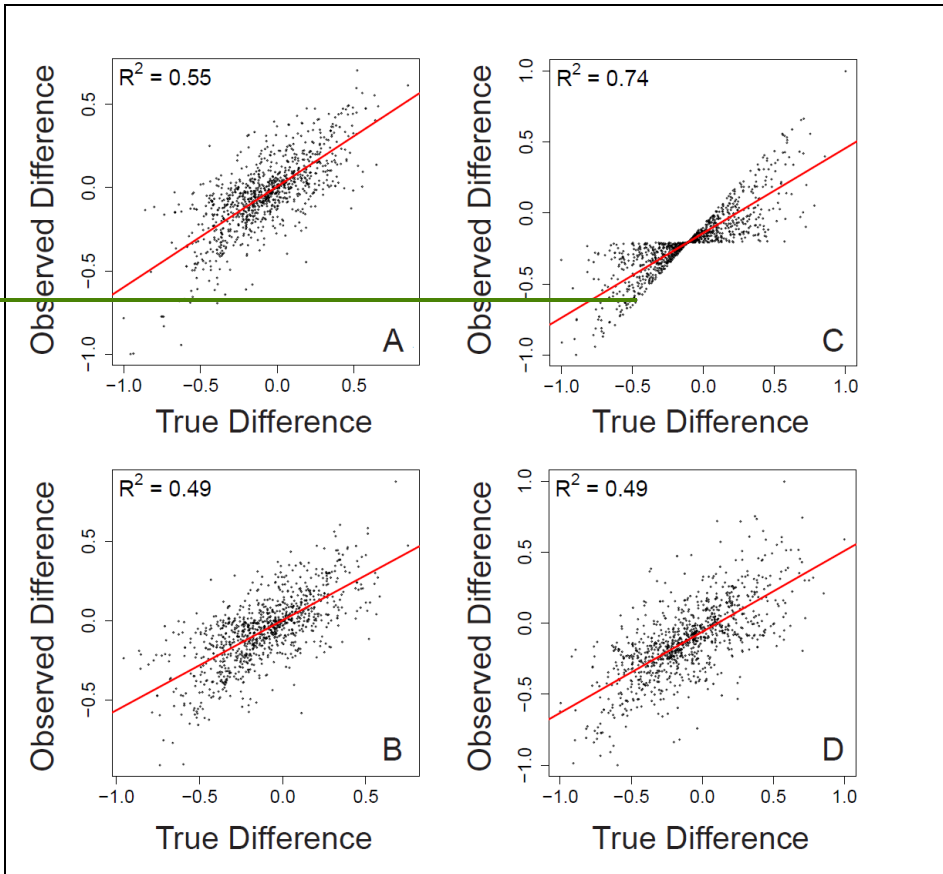


Figure 7. Variation in observed intensity explained by true abundance. Kernel density functions are shown for different relationships and types of error. Density functions were fit using R^2 values collated from across simulation iterations. Higher R^2 values indicate a stronger link (i.e., lower uncertainty) between observed intensities and true abundances. Black is for the relationship shown in Figure S1. Blue is for between-peak within sample differences (example relationships shown in Figures 8A,B). Gray is for within-peak between-sample differences when the same peak level error was used for both synthetic samples within a given simulation iteration (example relationship shown in Figure 8C). Red is for within-peak between-sample differences when different peak-level error was used across the synthetic samples within a given simulation iteration (example relationship shown in Figure 8D). While there are central tendencies in all four distributions, there is also significant variation in the degree to which observed intensities reflect true abundances. **Figure 7. Shannon α -diversity that includes simulated error regressed against true Shannon, across different scenarios.** (A) The same error applied to a given peak between samples, and 100 peaks per sample. (B) Different errors applied to a given peak between samples, and 100 peaks per sample. (C) The same error applied to a given peak between samples, and 1000 peaks per sample. (D) Different errors applied to a given peak between samples, and 1000 peaks per sample. On all panels the red line represents the one-to-one line and the dashed line is a spline fit to the data. All data are from the simulation model.



Formatted: Header

Formatted Table

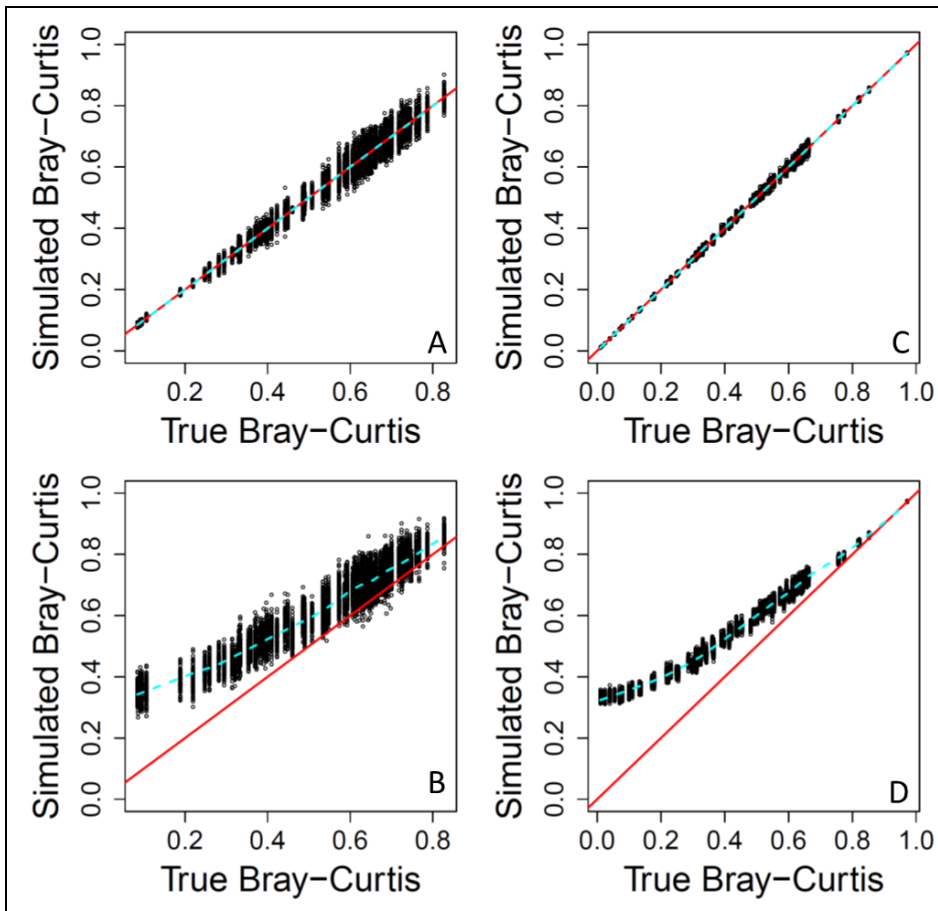
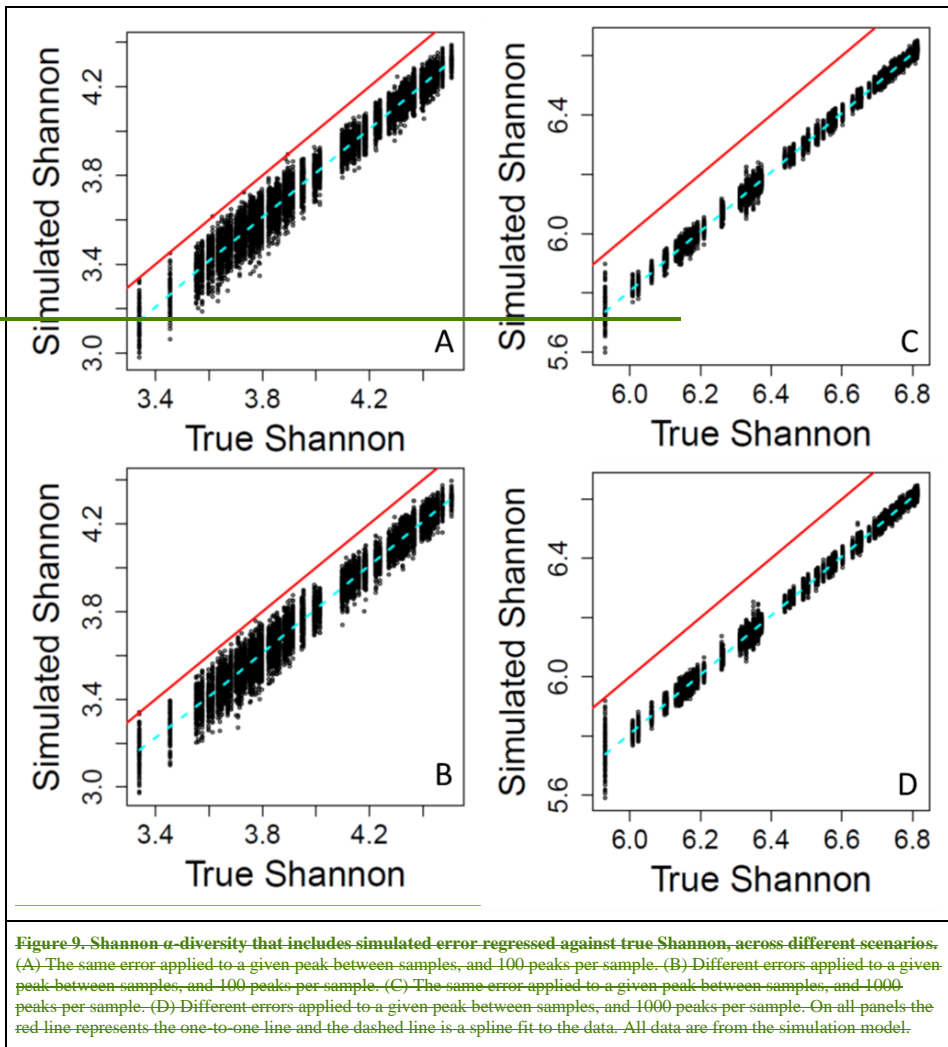
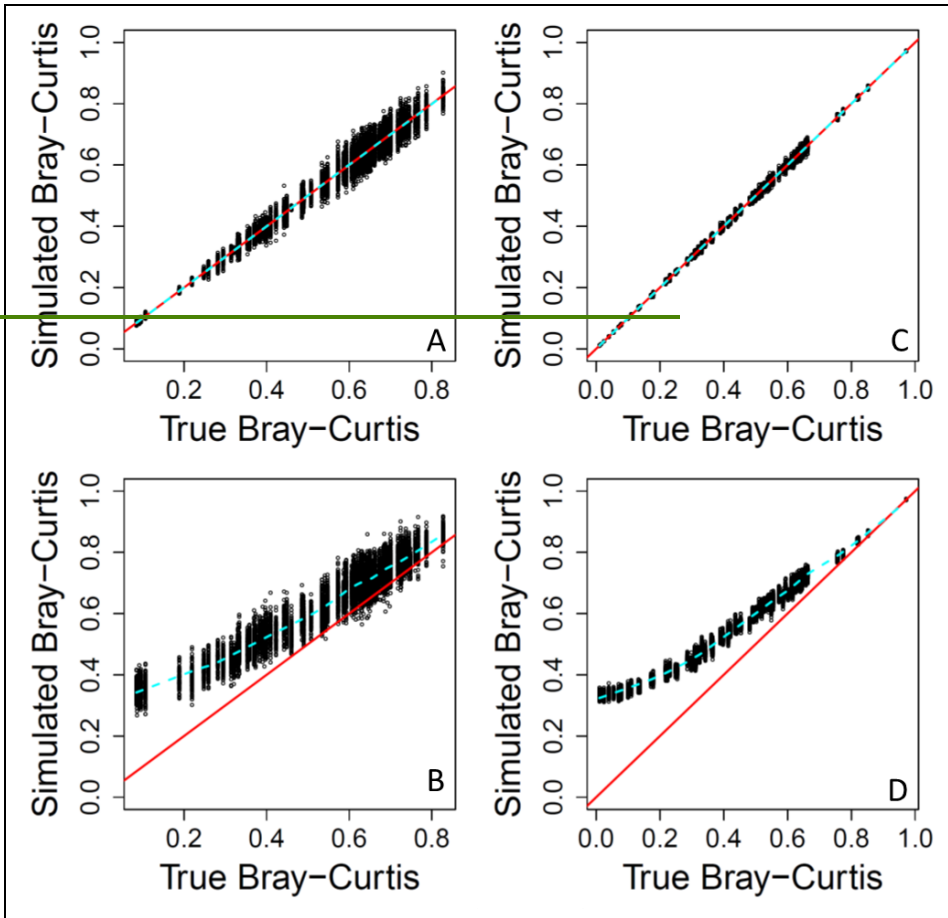


Figure 8. Observed differences in peak intensity Bray-Curtis dissimilarity as a function measure of β -diversity that includes simulated error regressed against true differences in peak intensity Bray-Curtis, across both within-peak and between-peak comparisons and across both kinds of error, different scenarios. (A) Between-peak differences with the same error applied to a given peak between samples, and 100 peaks per sample. (B) Between-peak differences with different errors applied to a given peak between samples, and 100 peaks per sample. (C) Within-peak differences with the same error applied to a given peak between samples, and 1000 peaks per sample. (D) Within-peak differences with different errors applied to a given peak between samples, and 1000 peaks per sample. On all panels the red line represents the linear regression one-to-one line and the dashed line is a spline fit to the data. All data are from the simulation model, and the associated R^2 value is provided.

Formatted: Font: Bold

Formatted: Font: Bold





Formatted: Header

Formatted Table

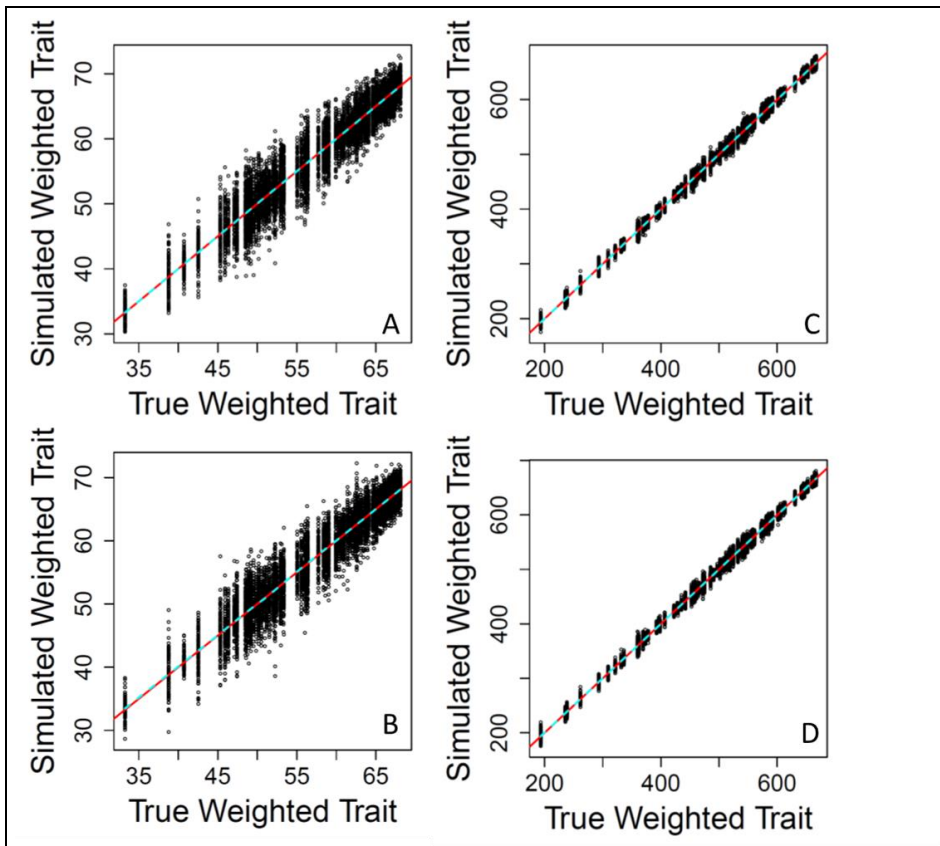


Figure 10. Bray-Curtis dissimilarity as a measure of β -diversity⁹. Mean peak-intensity-weighted trait values that include simulated error regressed against true Bray-Curtis mean peak-intensity-weighted trait values, across different scenarios. (A) The same error applied to a given peak between samples, and 100 peaks per sample. (B) Different errors applied to a given peak between samples, and 100 peaks per sample. (C) The same error applied to a given peak between samples, and 1000 peaks per sample. (D) Different errors applied to a given peak between samples, and 1000 peaks per sample. On all panels the red line represents the one-to-one line and the dashed line is a spline fit to the data. All data are from the simulation model.

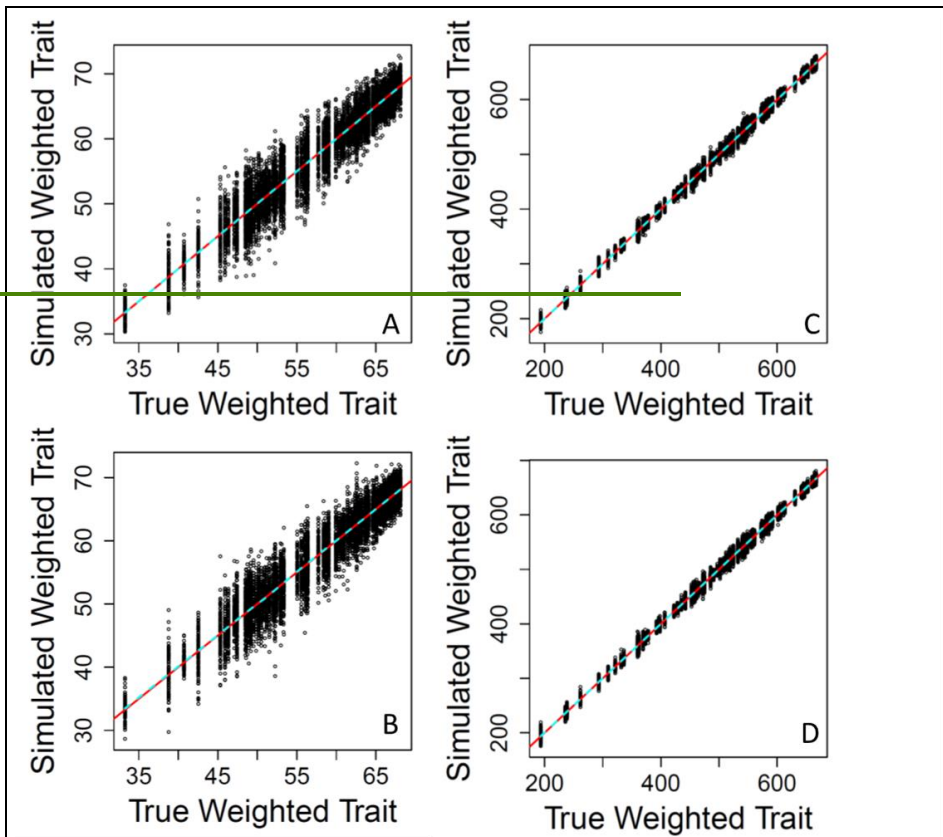


Figure 11. Mean peak-intensity-weighted trait values that include simulated error regressed against true mean peak-intensity-weighted trait values, across different scenarios. (A) The same error applied to a given peak between samples, and 100 peaks per sample. (B) Different errors applied to a given peak between samples, and 100 peaks per sample. (C) The same error applied to a given peak between samples, and 1000 peaks per sample. (D) Different errors applied to a given peak between samples, and 1000 peaks per sample. On all panels the red line represents the one-to-one line and the dashed line is a spline fit to the data. All data are from the simulation model.